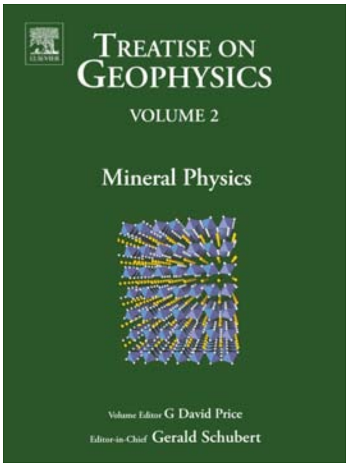
TREATISE ON
GEOPHYSICS
VOLUME 2
Mineral Physics
Volume Editor G David Price
Editor-in-Chief Gerald Schubert

2.02 Properties of Rocks and Minerals – Seismic Properties of Rocks and Minerals, and Structure of the Earth

L. Stixrude, University of Michigan, Ann Arbor, MI, USA

2.02.1 Introduction

The theoretical problem of computing the radial structure of a hydrostatic, gravitationally self-compressed body like Earth is well developed. In its simplest form, one solves the Poisson equation together with a constitutive relation for the variation of pressure and density with depth. While such solutions are important for our understanding of the structure of stars and giant planets, they have not played a major role in our understanding of Earth structure for at least two important reasons. First is the still overwhelming complexity of the constitutive relation in the case of the Earth and the other terrestrial planets. There are at least six essential elements and they are distributed inhomogeneously with depth, most evidently in the separation between the crust, mantle, and core. Moreover, there are more than 10 essential phases in the mantle alone, as compared with the single fluid phase that suffices in the case of the gas giants. Second is the power of seismological observations to reveal Earth structure. Adams and Williamson were able to estimate the radial density profile of Earth's mantle from a very different starting point, the observed variation of seismic wave velocities with depth, as embodied in their famous equation. The number and quality of seismic observations continues to grow as does our ability to interpret them, so that over the past few decades, seismologists have been able to constrain not only radial, but also lateral variations in seismic wave velocities and to produce three-dimensional (3-D) models of Earth structure.

One of the goals of geophysics is to relate the structure of Earth's interior as revealed primarily by seismology, to its thermal and chemical state, its dynamics and evolution. It is not generally possible to construct this more complete picture from knowledge of the seismologically revealed structure alone. The limitations are not so much practical – there is every indication that our knowledge of Earth structure will continue to improve for some time with further observation – but fundamental. The relationship of seismic wave velocity to composition and temperature cannot be inverted uniquely without further information.

Our primary interest in the seismic properties of Earth materials derives from this overarching goal, to place the current structural snapshot provided by seismology in the larger context of Earth evolution. Knowledge of material properties and behavior is the essential link between seismological observations and the temperature and composition of the interior. Indeed, the combination of geophysical observation and knowledge of materials properties derived from experimental and theoretical studies provide our most important constraints on the composition of the mantle and its thermal structure.

It is the aim of this contribution to illustrate the role of mineral physics as the interpretive link between seismic structure and dynamics, and to review what studies of material properties have taught us about the dynamics and composition of Earth. Our focus will be on Earth's mantle because the problem of determining the chemical and thermal state is particularly rich and because substantial progress has been made in the last decade.

The organization of this contribution takes its cue from Earth's seismic structure. We begin with a review of the 1-D elastic structure that accounts for most of the observed seismic signal. Special topics here will include the origin of high gradient zones and the origin of discontinuities. We continue with a discussion of lateral variations in seismic structure and their interpretation in terms of lateral variations in temperature, composition, and phase. A discussion of anisotropy will highlight the many important advances that have been made, particularly in our knowledge of the full elastic constant tensor of minerals, and also the formidable difficulties remaining, including a need for a better understanding of deformation mechanisms. We end with that part of Earth's seismic structure that is currently least amenable to interpretation, the anelastic part, indicating important developments in our understanding of the relevant material properties, and the gaps in our knowledge that remain.

2.02.2 Radial Structure

2.02.2.1 Overview

Perhaps the most remarkable and informative feature of Earth's radial structure is that it is not smooth (**Table 1**). The variation of seismic wave velocities with depth is broken up at several depths by rapid changes in physical properties. These are generally referred to as discontinuities, although in all probability, they represent regions where physical properties change very rapidly over a finite depth interval. Each discontinuity is associated with a mean depth, a range of depth due to topography on the discontinuity, and a contrast in physical properties, most directly the impedance contrast

$$\frac{\Delta I}{I} = \frac{\Delta \rho}{\rho} + \frac{\Delta V}{V} \quad [1]$$

where ρ is the density and V is either the shear or longitudinal-wave velocity and Δ represents the difference across the discontinuity. For isochemical changes in physical properties that follow Birch's law (Anderson *et al.*, 1968), the velocity contrast is approximately two-thirds of the impedance contrast for S-waves and approximately three-fourths for P-waves. Of the 14 discontinuities reported, some (e.g., 410, 660) are much more certain than others (e.g., 1200, 1700), both in terms of their existence and their properties.

Discontinuities are important because they tie seismological observations to the Earth's thermal and chemical state in an unusually precise and rich way. Many discontinuities in the mantle occur at depths that correspond closely to the pressure of phase transformations that are known from experiments to occur in plausible mantle bulk compositions (**Figure 1**). The pressure at which the phase transformation occurs generally depends on temperature via the Claussius–Clapeyron equation. The mean depth of a discontinuity then anchors the geotherm. Lateral variations in the depth of the discontinuity constrain lateral variations in temperature.

Phase transformations also influence mantle dynamics. For example, in a subducting slab, the perovskite forming reaction will be delayed as compared with the surroundings, tending to impede the slab's descent. The extent to which a phase transformation alters dynamics scales with the phase buoyancy parameter (Christensen and Yuen, 1985):

$$\Phi = \frac{\gamma \Delta \rho}{g \alpha \rho^2 h} \quad [2]$$

where γ is the Clapeyron slope, g is the acceleration due to gravity, α is the thermal expansivity, and h is the depth of the mantle. Phase transformations with negative Clapeyron slopes, such as the perovskite forming reaction, tend to impede radial mass transfer,

Table 1 Mantle discontinuities

Discontinuity	Depth (km)	Contrast	Affinity	References	Origin	References
Hales	59(12)	+7.0%	Global?	Revenaugh and Jordan (1991a, 1991b)	Anisotropy	Bostock (1998)
Gutenberg	77(14)	−9.0%	Oceans	Revenaugh and Jordan (1991a, 1991b)	Anisotropy	Gung, *et al.* (2003)
Lehmann	230(30)	+3.8%	Continents	Revenaugh and Jordan (1991a, 1991b)	Anisotropy	Gung, *et al.* (2003)
X	313(21)	+3.3%	Subduction	Revenaugh and Jordan (1991a, 1991b)	opx = hpcpx	Woodland (1998)
–	410(22)	+8.5%	Global	Flanagan and Shearer (1998), Dziewonski and Anderson (1981)	ol = wa	Ringwood and Major (1970)
–	520(27)	+3.0%	Global	Flanagan and Shearer (1998), Shearer (1990)	wa = ri	Rigden, *et al.* (1991)
–	660-	+8%?	Subduction	Simmons and Gurrola (2000)	ak = pv	Hirose (2002)
–	660(38)	+15.8	Global	Flanagan and Shearer (1998), Dziewonski and Anderson (1981)	ri = pv + mw	Ito and Takahashi (1989)
–	720(24)	+2.0	Global?	Revenaugh and Jordan (1991)	gt = pv	Stixrude (1997)
–	900(150)	?	Subduction?	Kawakatsu and Niu (1994)	Comp.?	Kawakatsu and Niu (1994)
–	1200	?	Global?	Vinnik, *et al.* (2001)	st = hy?	Karki, *et al.* (1997a, 1997b)
–	1700	?	?	Vinnik, *et al.* (2001)	capvc = capvt?	Stixrude, *et al.* (1996)
D″	2640(100)	+2.0%	Fast	Lay, *et al.* (1998b)	pv = ppv	Oganov and Ono (2004)
ULVZ	2870(20)	−10%	Slow	Garnero and Helmberger (1996)	melt	Williams and Garnero (1996)

Contrast is the S-wave impedance contrast, except for the D″ and ULVZ discontinuities (2640, 2870 km) which are reported as the S-wave velocity contrast. Value in parentheses following depth is the peak-to-peak (410, 520, 660), or rms (others) variation in the depth. The estimated impedance contrast at 660- is half of that of the 660 itself based on subequal reflectivity from 660- and 660 in the study of Simmons and Gurrola (2000). Affinity designations fast and slow refer to regions of anomalously high and low wave speeds in tomographic models, respectively. Origin designation ''comp.'' refers to a contrast in bulk composition possibly associated with subducted crust. Abbreviations capvc and capvt refer to the cubic and tetragonal phases of $CaSiO_3$ perovskite, respectively. Entries with a question mark are either unknown or uncertain.

while those with positive Clapeyron slopes, such as the olivine to wadsleyite transformation, tend to encourage it. In application to Earth's mantle, the phase buoyancy parameter must be generalized to account for the fact that only a fraction of the mantle undergoes the phase transformation (i.e., 50–60% in the case of the olivine to wadsleyite transition), and that nearly all phase transformations are at least divariant and occur over a finite range of depth.

Phase transformations also depend sensitively on bulk composition, which means that the Earth's discontinuity structure also constrains mantle chemistry. For example, the sequence of phase transformations with increasing pressure in olivine would be quite different if the mantle had twice as much FeO, and would no longer resemble the Earth's radial structure (Akaogi *et al.*, 1989).

Not all discontinuities can be explained by phase transformations. In some cases, no phase transformations occur near the appropriate depth. In others, phase transformations do occur, but the change in physical properties caused by the transition is far too subtle to explain the seismic signal. In the case of the D″ discontinuity, a phase transformation was only recently found that finally appears to explain most of the properties of this previously enigmatic

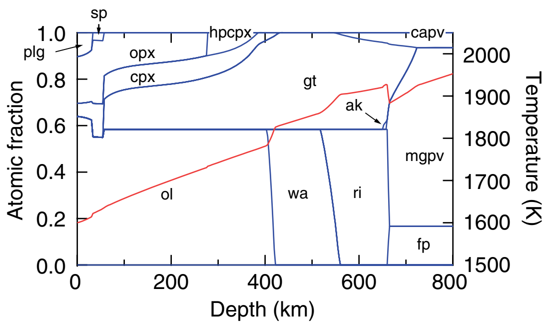

Figure 1 Phase proportions (blue, left axis) in a typical mantle bulk composition: Depleted MORB Mantle (DMM) of Workman and Hart (2005), along an isentrope (red, right axis) consistent with MORB genesis: potential temperature of 1600 K (Klein and Langmuir, 1987; McKenzie and Bickle, 1988). The isentrope and phase proportions are computed self-consistently from a unified thermodynamic formalism (Stixrude and Lithgow-Bertelloni, 2005a, 2005b). Phases are: plagiolcase (plg), spinel (sp), olivine (ol), orthopyroxene (opx), clinopyroxene (cpx), high-pressure Mg-rich clinopyroxene (hpcpx), garnet (gt), wadsleyite (wa), ringwoodite (ri), akimotoite (ak), Calcium silicate perovskite (capv), Magnesium silicate perovsite (pv), and ferropericlase (fp). From Stixrude L and Lithgow-Bertelloni C (2007) Influence of phase transformations on lateral heterogeneity and dynamics in Earth's mantle. *Earth and Planetary Science Letters*.

structure. Rapid variation with depth in chemical composition (e.g., the Moho), the pattern or strength of anisotropy, or in the magnitude of attenuation and dispersion may also cause discontinuities.

2.02.2.2 Upper Mantle

We take the upper mantle to be that region of the Earth between the Mohorovicic discontinuity and the 410 km discontinuity. This part of the Earth is challenging from a mineral physics point of view because heterogeneity, anisotropy, and attenuation are all large. Discussions of globally average radial structure are prone to mislead, which is why regional 1-D profiles, as well as 3-D tomographic models are important to keep in mind. This part of the Earth is remarkably rich in structure with features that have resisted explanations in terms of mineralogical models.

One of the most remarkable features of upper mantle structure is the presence of a low velocity zone (Gutenberg, 1959). A pattern of decreasing velocity with increasing depth appears unique to the boundary layers of the mantle (see also discussion of D″ below). The low velocity zone is more prominent under oceans than under continents; and is more prominent under young oceanic lithosphere than old (Anderson, 1989).

The origin of the low velocity zone is readily understood in terms of Earth's thermal state and the properties of minerals. Negative velocity gradients will appear whenever the thermal gradient exceeds a critical value such that the increase of velocity with compression is overcome by the decrease of velocity on heating (Anderson *et al.*, 1968; Birch, 1969). The critical thermal gradient

$$\beta_S = -\left(\frac{\partial V_S}{\partial P}\right)_T \bigg/ \left(\frac{\partial V_S}{\partial T}\right)_P \qquad [3]$$

for shear waves is modest: 2 K km^{-1} for olivine. One then expects negative velocity gradients to be widespread in the shallow upper mantle on the basis of heat flow observations. There is a critical thermal gradient for the density as well

$$\beta_\rho = \frac{1}{\alpha K_T} \qquad [4]$$

where α is the thermal expansivity and K_T is the isothermal bulk modulus, which is just the inverse of the thermal pressure gradient that has been discussed by Anderson (Anderson, 1995). The value for olivine $\sim$10 K km^{-1}, is less than that in most of the Earth's upper thermal boundary layer. The low velocity zone should be associated with locally unstable stratification in which more dense material overlies less dense material.

Comparison to the critical thermal gradient also explains much of the lateral variations in the structure of the low velocity zone. In the half-space cooling model of mantle, the geothermal gradient decreases with lithospheric age, producing a weaker negative velocity gradient as seen seismologically (Graves and Helmberger, 1988; Nataf *et al.*, 1986; Nishimura and Forsyth, 1989). Under continents, the geothermal gradient is much less steep, but even under cratons exceeds the critical value; for example, the gradient is 4 K km^{-1} under the Abitibi province (Jaupart and Mareschal, 1999). Indeed, the low velocity zone appears to be much less prominent, but not absent under some continental regions (Grand and Helmberger, 1984).

Are other factors required to quantitatively explain the values of the lowest velocities seen in the low velocity zone? It has long been suggested that partial melt may be present in this region of the mantle (Anderson and Sammis, 1969; Birch, 1969; Green and Liebermann, 1976; Lambert and Wyllie, 1968; Ringwood, 1969; Sato *et al.*, 1989). While partial melt is not required to explain the existence of a low velocity zone *per se* as the argument regarding the critical thermal gradient above demonstrates, it is difficult to rule out its presence on the basis of quantitative comparisons of seismological observations to the elastic properties of upper mantle assemblages. Recent such comparisons have concluded that partial melt is not required to explain the seismological observations, except in the immediate vicinity of the ridge (Faul and Jackson, 2005; Stixrude and Lithgow-Bertelloni, 2005a) (**Figure 2**). These studies also find it essential to account for the effects of attenuation and dispersion, which is unusually large in this region (see below).

The low velocity zone has sometimes been seen as being bounded above by the Gutenberg (G) discontinuity near 65 km. This discontinuity has also been associated with the base of the lithosphere. The impedance contrast is variable, large, and negative, that is, velocities are less below the transition (Gaherty *et al.*, 1999a; Revenaugh and Jordan, 1991b). Phase transformations occurring near this depth do not produce velocity discontinuities of nearly sufficient magnitude, or even the right sign. A rapid change in attenuation produces a velocity change of the right sign (Karato and Jung, 1998), but far too small in magnitude (Stixrude and Lithgow-Bertelloni, 2005a). A rapid change in partial melt fraction, from a melt-free lithosphere to a partially molten low velocity zone, also produces a velocity change that is too small as modeling indicates that the discontinuity is made up equally of anomalously high velocity above the discontinuity and anomalously low velocity below (Stixrude and Lithgow-Bertelloni, 2005a) (**Figure 2**).

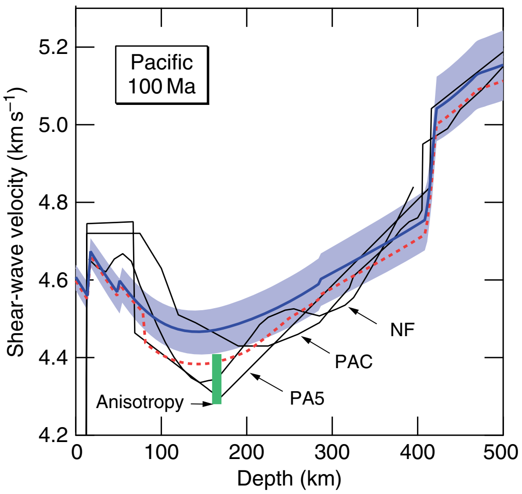

Figure 2 The shear-wave velocity of pyrolite along a 100 Ma conductive cooling geotherm in the elastic limit (bold line), and including the effects of dispersion according to the seismological attenuation model QR19 (Romanowicz, 1998) and $\alpha = 0.25$ (bold dashed). The shading represents the uncertainty in the calculated velocity. The mineralogical model is compared with seismological models (light lines) PAC (Graves and Helmberger, 1988), NF110+ (Nishimura and Forsyth, 1989), and PA5 (Gaherty, *et al.*, 1999a). The approximate magnitude of SH–SV anisotropy is indicated by the vertical bar. From Stixrude L and Lithgow-Bertelloni C, (2005a) Mineralogy and elasticity of the oceanic upper mantle: Origin of the low-velocity zone *Journal of Geophysical Research*, *Solid Earth* 110: B03204 (doi:10.1029/2004JB002965).

The Lehmann discontinuity, near 200 km depth, also does not have a counterpart in mantle phase transformations. In some global models (Dziewonski and Anderson, 1981) this discontinuity is enormous, exceeding in magnitude the much more widely studied 410 km discontinuity. The Lehmann discontinuity is observed preferentially under continents (Gu *et al.*, 2001), while the G discontinuity is found preferentially under oceans (Revenaugh and Jordan, 1991b). It has been proposed that the Lehmann discontinuity represents a change in anisotropy caused by a change in the dominant deformation mechanism from dislocation dominated to diffusion dominated creep (Karato, 1992). The Lehmann and Gutenberg discontinuities may actually be the same feature, occurring at shallower depths under oceans and greater depths under continents. Both may be caused by a change in anisotropy via a change in the pattern of preferred orientation associated with the base of the lithosphere and a transition to more deformable asthenosphere where preferred orientation is more likely to develop (Gung *et al.*, 2003) (**Figure 3**). This model is in apparent disagreement with those based on ScS reverberation, which require an increase in SV with increasing depth across the Lehmann (Gaherty and Jordan, 1995; Revenaugh and Jordan, 1991b).

A smaller discontinuity is seen locally called the X discontinuity near 300 km depth (Revenaugh and Jordan, 1991b). A phase transition appears to be the most likely explanation (Woodland, 1998), involving a subtle modification of the orthopyroxene structure to a slightly denser monoclinic form with the same space group as diopside (clinopyroxene) (Angel *et al.*, 1992; Pacalo and Gasparik, 1990) (**Figure 1**). The elastic properties of this unquenchable high pressure phase have only recently been measured and appear to confirm the connection to the seismic discontinuity (Kung *et al.*, 2005). The velocity contrast

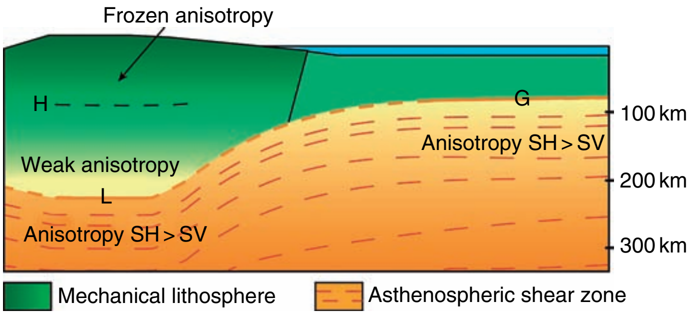

Figure 3 Sketch illustrating the pattern of anisotropy found in a recent tomographic model in relation to lithospheric thickness, and to the Lehmann (L) and Gutenberg (G) discontinuities. The Hales discontinuity (H) is also indicated. From Gung YC, Panning M, and Bomanowicz B (2003) Global anisotropy and the thickness of continents. *Nature* 422: 707–711.

in the pure composition is 8%, reduced to less than 0.5% in a typical pyrolite composition along a normal mantle geotherm (Stixrude and Lithgow-Bertelloni, 2005a). The proportion of orthopyroxene, and thus the magnitude of the velocity change, should increase with decreasing temperature and with depletion; indeed, the X discontinuity is preferentially observed near subduction zones.

The velocity gradient between the low velocity zone and the 410 km discontinuity is very large (**Figure 2**). In some regional models, the gradient exceeds that of the transition zone (Gaherty *et al.*, 1999a; Graves and Helmberger, 1988; Nishimura and Forsyth, 1989). According to the usual Bullen analysis, this means that this region is either nonadiabatic, or inhomogeneous in bulk composition or phase (Stixrude and Lithgow-Bertelloni, 2005a). In this context, it is important to remind ourselves that when we discuss radial gradients in velocities, we are not discussing seismological observations, but rather nonunique models that are consistent with those observations. An approach that has seen only little application to date is the direct comparison of mineralogical models of mantle structure with the seismological observations themselves. This could be accomplished, for example, in the manner of a hypothesis test: computing seismological observables (e.g., body wave travel times and normal mode frequencies) from a mineralogical model and comparing with the observations. It is probably only through approaches like these that many of the more difficult issues in upper mantle structure will be resolved.

2.02.2.3 Transition Zone

This region is so named because of the phase transformations that were anticipated and subsequently found to take place within it. While phase transformations are not restricted to the transition zone as our discussion of the upper and lower mantles make clear, the two largest ones in terms of changes in physical properties do occur here. This region encompasses the transformation of the mantle from uniformly fourfold to uniformly sixfold coordinated silicon.

The two largest discontinuities in the mantle occur at 410 and 660 km depth. These have been explained by phase transformations from olivine to its high pressure polymorph wadsleyite for the 410 (Ringwood and Major, 1970) and from ringwoodite, the next highest pressure olivine polymorph, to the assemblage perovskite plus periclase for the 660 according to the reaction (Liu, 1976)(**Figure 1**).

$$\mathrm{Mg_2SiO_4\,(ringwoodite)} = \mathrm{MgSiO_3\,(perovskite)} + \mathrm{MgO\,(periclase)} \qquad [5]$$

These explanations have received considerably scrutiny over the past several years and have held up well. In addition to the issues discussed in more detail below has been vigorous debate concerning the pressure at which the two transformations occur and whether these in fact match the depth of the discontinuities (Chudinovskikh and Boehler, 2001; Fei *et al.*, 2004; Irifune *et al.*, 1998; Shim *et al.*, 2001), and whether the Clapeyron slope of the transitions can account for the seismologically observed topography on the discontinuities (Helffrich, 2000).

In the case of the 410 km discontinuity, the magnitude and the sharpness of the velocity jump have also been the subject of considerable debate. Several studies have argued that the magnitude of the velocity change at the olivine to wadsleyite transition in a typical pyrolitic mantle composition is too large and that the mantle at this depth must have a relatively olivine poor bulk composition (Duffy *et al.*, 1995; Gwanmesia *et al.*, 1990; Li *et al.*, 1998; Liu *et al.*, 2005; Zha *et al.*, 1997). Phase equilibrium studies (Akaogi *et al.*, 1989; Frost 2003; Katsura and Ito, 1989; Katsura *et al.*, 2004) have shown that the olivine to wadsleyite transition in the binary Mg_2SiO_4–Fe_2SiO_4 system occurs over a depth range too wide to account for the observed reflectivity of this transition, at frequencies as high as 1 Hz (Benz and Vidale, 1993).

There have been several proposals to explain the apparent discrepancy in sharpness (Fujisawa, 1998; Solomatov and Stevenson, 1994). Perhaps the simplest recognizes that the mantle is not a binary system: chemical exchange of olivine and wadsleyite with nontransforming phases sharpens the transition considerably (Irifune and Isshiki, 1998; Stixrude, 1997) (**Figure 4**). Nonlinearities inherent in the form of coexistence loops also tend to sharpen the transition (Helffrich and Bina, 1994; Helffrich and Wood, 1996; Stixrude, 1997). Modeling of finite frequency wave propagation shows that the form of the transition predicted by equilibrium thermodynamics and a pyrolitic bulk composition can account quantitatively for the observations (Gaherty *et al.*, 1999b). This study also shows that when the shape of the transition is properly accounted for, the magnitude of the velocity jump in pyrolite is consistent with those observations most sensitive to it, that is, the reflectivity.

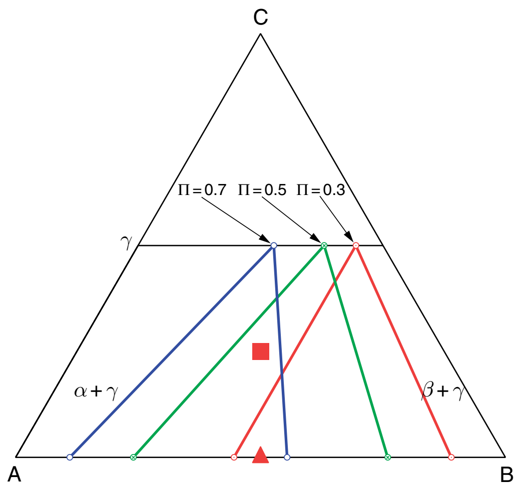

Figure 4 The influence of nontransforming phase(s) (γ) on the sharpness of the transformation from phase α to phase β. Colored lines indicate the compositions of the three coexisting phases with increasing scaled pressure (Π) within the coexistence interval. When the bulk composition lies on the A–B join, the transition is broad: the bulk composition represented by the solid triangle lies within the coexistence region over the entire pressure range shown ($\Pi = 0.3$–0.7). When component C is added, the transition occurs over a narrower pressure interval: the bulk composition represented by the solid square lies within the coexistence region over a fraction of the pressure range shown ($\Pi = 0.5$–0.7). After Stixrude L (1997) Structure and sharpness of phase transitions and mantle discontinuities. *Journal of Geophysical Research*, *Solid Earth* 102: 14835–14852.

The detailed form of the 410 km discontinuity may become a very sensitive probe of mantle conditions. The width of the discontinuity is found to increase with decreasing temperature (Katsura and Ito, 1989), which would affect the visibility of transition (Helffrich and Bina, 1994). Phase equilibria depend strongly on iron content such that the transition is broadened with iron enrichment. Iron enrichment beyond $x_{Fe} = 0.15$ at normal mantle temperatures causes the transition to become univariant (infinitely sharp in a pure olivine composition), with ringwoodite coexisting with olivine and wadsleyite (Akaogi *et al.*, 1989; Fei *et al.*, 1991). The transition is also sensitive to water content as wadsleyite appears to have a much higher solubility than olivine (Wood, 1995) although more recent results suggest that water partitioning between these two phases, and the influence of water on the form of the 410, is not as large as previously assumed (Hirschmann *et al.*, 2005). Portions of the mantle are found to have broad and nonlinear 410 discontinuities, consistent with the anticipated effects of water enrichment (van der Meijde *et al.*, 2003).

In some locations, the 410 is overlain by low velocity patches that have been interpreted as regions of partial melt, perhaps associated with water enrichment. These patches appear to be associated with subduction zones, suggesting the slab as a possible source of water (Obayashi *et al.*, 2006; Revenaugh and Sipkin 1994; Song *et al.*, 2004). Other interpretations involving much more pervasive fluxing of water through the transition zone have also been advanced (Bercovici and Karato, 2003), although it has been argued that this scenario is inconsistent with the thermodynamics of water-enhanced mantle melting (Hirschmann *et al.*, 2005). Measurements of the density of hydrous melt at the pressure of the 410 indicate that it may be gravitationally stable (Matsukage *et al.*, 2005; Sakamaki *et al.*, 2006).

Initial studies of the influence of iron on the ringwoodite to perovskite plus periclase transition also seemed to indicate that this transition was too broad to explain reflectivity observations (Jeanloz and Thompson, 1983; Lees *et al.*, 1983). But in a seminal study Ito and Takahashi (1989) showed that this transition was remarkably sharp, occurring over a pressure range less than experimental resolution (0.1 GPa). The unusual sharpness was subsequently explained in terms of Mg–Fe partitioning and nonideal Mg–Fe mixing in the participating phases (Fei *et al.*, 1991; Wood, 1990). While the central result of Ito and Takahashi's study remains unchallenged, it will be important to replicate these results in realistic mantle compositions (Litasov *et al.*, 2005), and to further explore the thermochemistry of the phases involved.

Recent studies have indicated complexity in the structure of the 660 (**Figure 5**). In relatively cold mantle, the transition (eqn [5]) is preceded by (Weidner and Wang, 1998)

$$MgSiO_3\,(\text{akimotoite}) = MgSiO_3\,(\text{perovskite}) \qquad [6]$$

while in hot mantle the amount of ringwoodite is diminished prior to the transition (eqn [5]) via (Hirose, 2002)

$$Mg_2SiO_4\,(\text{ringwoodite}) = MgSiO_3\,(\text{majorite}) + MgO\,(\text{periclase}) \qquad [7]$$

In cold and hot mantle, the reactions (eqns [5]–[7]) will be followed by a further reaction

$$MgSiO_3\,(\text{majorite}) = MgSiO_3\,(\text{perovskite}) \qquad [8]$$

The sequence of reactions [5] and [6] should produce a 'doubled' 660 in which a single velocity jump is replaced by two that are closely spaced in depth and of similar magnitude. There is some seismological evidence for this doubling in some locations (Simmons and Gurrola, 2000). The relative importance of reactions [5]–[8] will also depend on the bulk composition, particularly the Al content (Weidner and Wang, 1998).

Below 660 is a steep velocity gradient that may be considered a continuation of the transition zone. This feature is seen in mineralogical models as the signature of the garnet to perovskite transition (eqn [8]), which is gradual and spread out over more than 100 km (Weidner and Wang, 1998). The gradual nature of this transition, as opposed to the much sharper ones discussed so far, is readily understood. The difference in composition between Al-rich garnet, and relatively Al-poor perovskite is large, and this creates a broad pressure–composition coexistence region (phase loop)

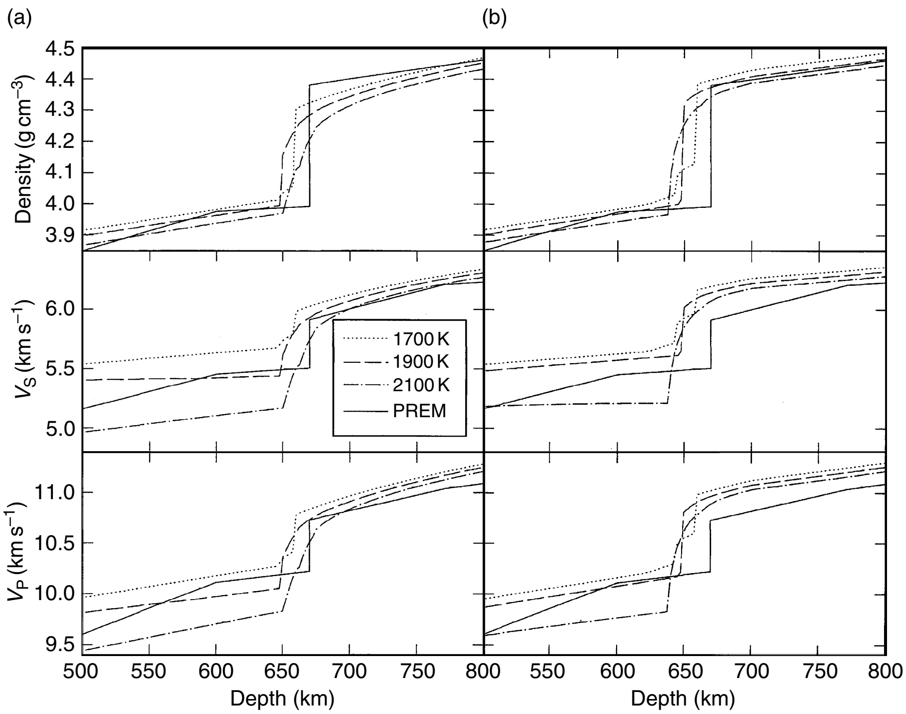

Figure 5 Calculated density and elastic wave velocities for different geotherms for pyrolite-like compositions with (a) 3% Al_2O_3 and (b) 5% Al_2O_3. Calculations are compared with the PREM seismological model (Dziewonski and Anderson, 1981). From Weidner DJ and Wang YB (1998) Chemical- and Clapeyron-induced buoyancy at the 660 km discontinuity. *Journal of Geophysical Research*, *Solid Earth* 103: 7431–7441.

(Akaogi *et al.*, 2002; Hirose *et al.*, 2001). Although it is broad, this transition may be responsible for a seismic discontinuity seen in some studies near 720 km depth (Deuss *et al.*, 2006; Revenaugh and Jordan, 1991b; Stixrude, 1997). Apparent bifurcation of the 660 may then have two distinct sources: eqns [5] and [6] in cold mantle, and eqns [5] and [8] in hotter mantle. It is conceivable that three reflectors may be observable in cold mantle (eqns [5], [6], and [8]), although this has not yet been seen.

The 520 km discontinuity is seen in global stacks of SS precursors (Shearer, 1990); there is evidence that it is only regionally observable (Gossler and Kind, 1996; Gu *et al.*, 1998; Revenaugh and Jordan, 1991a). Phase transformations that may contribute to this discontinuity include wadsleyite to ringwoodite (Rigden *et al.*, 1991) and the exsolution of calcium perovskite from garnet (Ita and Stixrude, 1992; Koito *et al.*, 2000). Both of these transitions are broad, which may account for the intermittent visibility of the 520. Seismological evidence for doubling of this discontinuity in some regions has renewed interest in the structure and sharpness of these transitions (Deuss and Woodhouse, 2001). The 520 km discontinuity has also been attributed to chemical heterogeneity, possibly associated with subduction (Sinogeikin *et al.*, 2003).

In addition to velocity discontinuities, the transition zone is distinguished by an unusually large velocity gradient, which exceeds that of any individual transition zone phase (**Figure 6**). Most explanations have focused on the series of phase transformations that occur in the transition zone as the cause of this gradient. These include not only those already mentioned in connection with discontinuities, but also broader features such as the dissolution of pyroxenes into garnet. The standard model, that the transition zone is adiabatic and chemically homogeneous with a pyrolitic composition, has been tested successfully against seismological constraints on the bulk sound velocity (Ita and Stixrude, 1992). Quantitative tests against the longitudinal- and shear-wave velocity are still hampered by uncertainties in the physical properties of key phases, particularly garnet-majorite (Liu *et al.*, 2000; Sinogeikin and Bass, 2002) and $CaSiO_3$ perovskite.

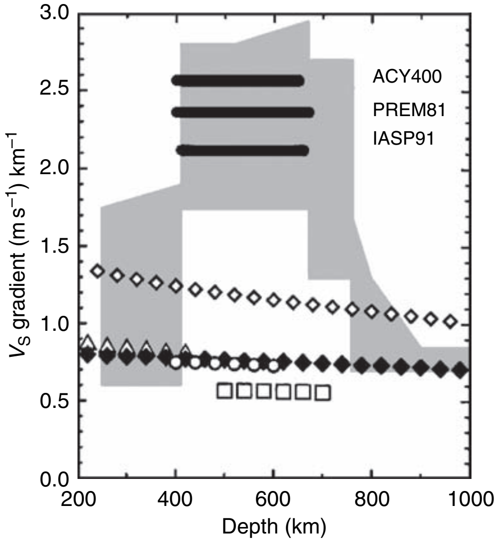

Figure 6 The velocity gradient from seismic studies and mineral physics. The shaded area is from Kennett (1993). The average gradients from global seismic models PREM81, ACY400, IASP91 (Dziewonski and Anderson, 1981; Kennett and Engdahl, 1991; Montagner and Anderson, 1989) are shown by horizontal solid lines. Solid diamonds are extrapolation of Brillouin spectroscopy data on a garnet of 1:1 majorite:pyrope composition, and open diamonds are an extrapolation of data of (Liu, *et al.*, 2000) on the same composition. Triangles – olivine, circles – wadsleyite, squares – ringwoodite. All velocity extrapolations are done along a 1673 K adiabat. From Sinogeikin SV and Bass JD (2002) Elasticity of majorite and a majorite–pyrope solid solution to high pressure: Implications for the transition zone. *Geophysical Research Letters* 29: 1017 (doi:10.1029/2001GL013937).

2.02.2.4 Lower Mantle

The most prominent seismic anomaly in the lower mantle is the division between the D″ layer and the rest. The D″ layer is distinguished by a change in radial velocity gradient, and a velocity discontinuity at its top (Lay and Helmberger, 1983). The velocity discontinuity is prominent where it is seen, although it is not present everywhere and is larger in S than in P (Lay *et al.*, 1998a; Wysession *et al.*, 1998; Young and Lay, 1987). Below this discontinuity most models show velocity decreasing with increasing depth: the D″ represents the mantle's second low velocity zone. In analogy with that in the shallow mantle, the D″ velocity gradient may also be caused by superadiabatic temperature gradients associated with the lower dynamical boundary layer of mantle convection.

Mineralogical explanations of the D″ discontinuity now focus on the transformation from $MgSiO_3$ perovskite to the postperovskite phase (**Figure 7**) (Murakami *et al.*, 2004; Oganov and Ono, 2004; Tsuchiya *et al.*, 2004a). The transition appears to

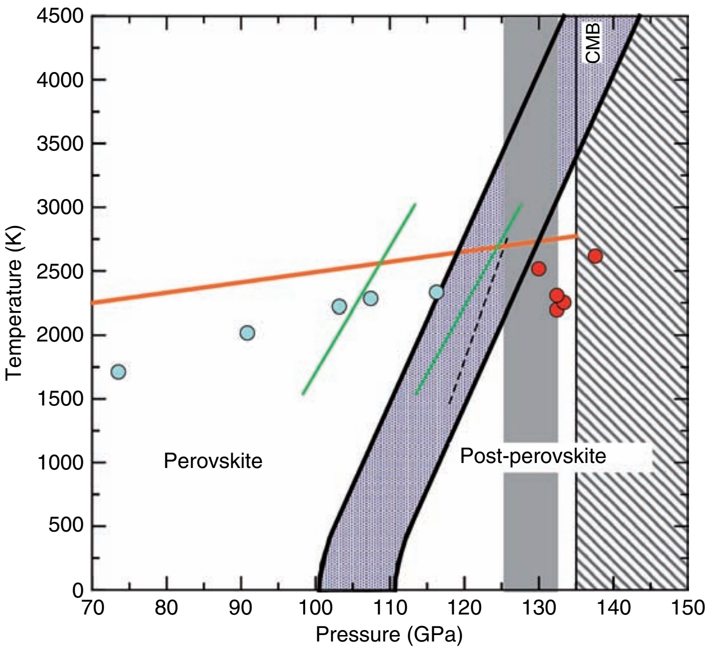

Figure 7 Post-perovskite transition from Tsuchiya *et al*. (2004a) (blue band), and Oganov and Ono (2004) (green lines) with lower (LDA) and upper (GGA) bounds, compared with experiment (Murakami, *et al*., 2004) (blue circles: pv, red circles: ppv), and the Clapeyron slope inferred from D″ topography (Sidorin, *et al*., 1999) (dashed), a mantle geotherm (orange) (Brown and Shankland, 1981) and the pressure range of D″ topography (gray shading) (Sidorin, *et al*., 1999). After Tsuchiya T, Tsuchiya J, Umemoto K, and Wentzcovitch RM (2004a) Phase transition in $MgSiO_3$ perovskite in the earth's lower mantle *Earth and Planetary Science Letters* 224: 241–248.

occur at the right pressure and to have the right Clapeyron slope to explain the intermittent visibility. Predictions of the elastic constants show a larger contrast in V_S than in V_P, consistent with most seismological observations of the discontinuity (Iitaka *et al*., 2004; Tsuchiya *et al*., 2004b; Wentzcovitch *et al*., 2006). Indeed, a phase transformation with very similar properties was anticipated on the basis of a combined seismological and geodynamical study (Sidorin *et al*., 1999).

The ultralow velocity zone is a narrow intermittent layer less than 40 km thick with longitudinal-wave velocities approximately 10% lower than that of the rest of D″ (Garnero and Helmberger, 1996). It is still unclear what could cause such a large anomaly. A search for explanations is hampered by uncertainties concerning the relative magnitude of density and longitudinal and shear velocity anomalies. Many studies have focused on the possibility of partial melt in this region (Stixrude and Karki, 2005; Williams and Garnero, 1996). Others have emphasized the role of iron enrichment, possibly related to chemical reaction between mantle and core (Garnero and Jeanloz, 2000), or subduction (Dobson and Brodholt, 2005). In this view the ultralow velocity zone may be more properly regarded as the outermost layer of the core, rather than the bottom-most layer of the mantle (Buffett *et al*., 2000).

There have been persistent reports of reflection or scattering from within the lower mantle (Castle and van der Hilst, 2003; Deuss and Woodhouse, 2002; Johnson, 1969; Kaneshima and Helffrich, 1998; Kawakatsu and Niu, 1994; Lestunff, *et al*., 1995; Paulssen, 1988; van der Meijde *et al*., 2005; Vinnik *et al*., 2001). These are only locally observed, and so may either be associated with chemical heterogeneity, possibly related to subduction (Kaneshima and Helffrich, 1998; Kawakatsu and Niu, 1994), or a phase transition that has either a weak velocity signal or a large Clapeyron slope. Phase transformations that are expected to occur in the lower mantle and that are associated with significant velocity anomalies include (**Figure 8**): (1) Phase transformations in silica, from stishovite, to $CaCl_2$ to α-PbO_2 structured phases (Carpenter *et al*., 2000; Karki *et al*., 1997b). Free silica would be expected only in enriched compositions, such as deeply subducted oceanic crust. The first of these transitions has

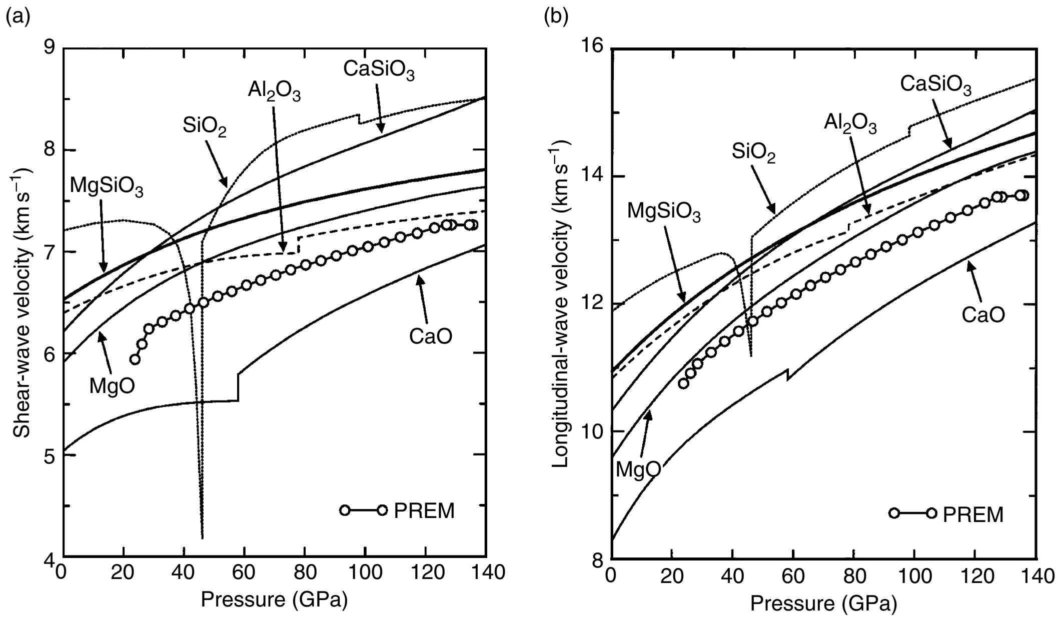

Figure 8 Comparisons of the static shear (a) and longitudinal (b) wave velocities of lower mantle minerals computed via density functional theory compared with the PREM model (Dziewonski and Anderson, 1981). The discontinuous changes in SiO_2 are caused by phase transformations from stishovite to the $CaCl_2$ structure (45 GPa) and then to the α-PbO_2 structure (100 GPa). After Karki BB and Stixrude L (1999) Seismic velocities of major silicate and oxide phases of the lower mantle. *Journal of Geophysical Research* 104: 13025–13033.

a particularly large elastic anomaly. (2) A phase transformation in calcium perovskite from tetragonal to cubic phases (Stixrude *et al.*, 1996).

2.02.2.5 Core

It is known that the properties of the outer core do not match those of pure iron, which is significantly denser (Birch, 1964; Brown and McQueen, 1986). The search for the light element is still in its infancy, with the number of candidate light elements seeming to grow, rather than narrow with time (Poirier, 1994). It has been pointed out that there is no *a priori* reason to believe that the composition of the core is simple or that it contains only one or a few elements other than iron (Stevenson, 1981). In any case, further experimental and theoretical constraints on the phase diagrams and physical properties of iron light element systems will be essential to the solution.

Two relatively new approaches to constraining the nature and amount of light element in the core show considerable promise. The first relates the partitioning of candidate light elements between solid and liquid phases to the density contrast at the inner-core boundary (Alfe *et al.*, 2002a). While sulfur and silicon are found to partition only slightly, producing a density jump that is too small, oxygen strongly favors the liquid phase, producing a density jump that is too large. Within the accuracy of the theoretical calculations used to predict the partitioning, this study then appears to rule out either of these three as the sole light element in the inner core, and suggests a combination of oxygen with either silicon or sulfur as providing a match to the seismologically observed properties. Another approach is to test core formation hypotheses via experimental constraints on element partitioning between core and mantle material. In the limit that proto-core liquid approached equilibrium with the mantle as it descended, experiments point to sulfur as the only one sufficiently siderophile to remain in significant amounts in iron at pressures thought to be representative of core formation (~30 GPa) (Li and Agee, 1996). On the other hand, experimental simulations of the core–mantle boundary (136 GPa) show substantial reaction between core and mantle material and incorporation of large amounts of Si and O in the metal (Knittle and Jeanloz, 1989; Takafuji *et al.*, 2005) (**Figure 9**).

The temperature in the core may be constrained by the melting temperature of iron and iron alloys.

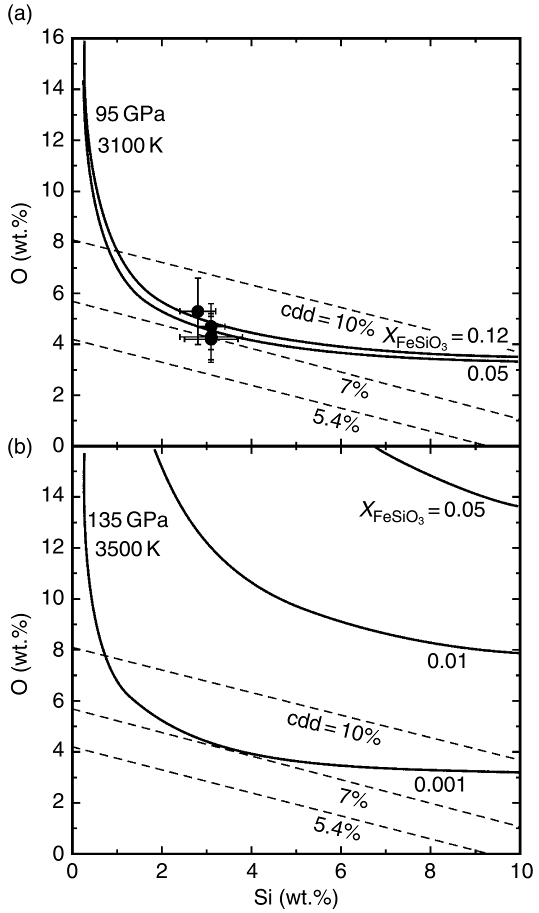

Figure 9 The simultaneous solubilities of O and Si in liquid iron in equilibrium with (Mg, Fe)SiO_3 perovskite. Solid curves represent values calculated from a thermodynamic model at (a) 95 GPa and 3100 K and (b) 135 GPa and 3500 K as a function of $FeSiO_3$ component in coexisting perovskite (X_{FeSiO3}). The model is constrained by experimental measurements, a subset of which are shown in (a) at 93–97 GPa and 3050–3150 K in contact with (Mg, Fe)SiO_3 perovskite ($X_{FeSiO3} = 0.04$–0.12) (circles). The broken lines show the amounts of O and Si that are required to account for a core density deficit (cdd) relative to pure iron of 10%, 7%, and 5.4% (Anderson and Isaak, 2002). From Takafuji N, Hirose K, Mitome M, and Bando Y (2005) Solubilities of O and Si in liquid iron in equilibrium with (Mg, Fe)SiO_3 perovskite and the light elements in the core. *Geophysical Research Letters* 32: L06313 (doi:10.1029/2005GL022773).

Consensus has been building in recent years on the melting temperature of pure iron near the inner-core boundary. First-principles theory (Alfe *et al.*, 2002b) and temperature measurements in dynamic compression (Nguyen and Holmes, 2004), both converge on the melting temperature proposed by Brown and McQueen (1986) on the basis of dynamic compression and modeled temperatures. The largest remaining uncertainty appears to be the influence of the light element on the melting temperature. Density functional theory predicts freezing point depression of 700 K for light element concentrations required to match the density deficit (Alfe *et al.*, 2002a), similar to estimates based on the van Laar equation (Brown and McQueen, 1982). An alternative approach to estimating the temperature at Earth's center is to compare the elasticity of iron to that of the inner core. This leads to an estimate of 5400 K at the inner-core boundary, consistent with estimates based on melting temperatures (Steinle-Neumann *et al.*, 2001).

The outer core is homogeneous and adiabatic to within seismic resolution (Masters, 1979) and represents possibly the clearest opportunity for estimating the temperature increment across any layer in the Earth. The adiabatic temperature gradient

$$\left(\frac{\partial \ln T}{\partial P}\right)_S = \frac{\gamma}{K_S} \qquad [9]$$

depends on K_S, which is known as a function of depth from seismology, and the Grüneisen parameter γ, which has been measured for pure iron (Brown and McQueen, 1986). Integrating this equation across the outer core produces a temperature difference of 1400 K (Steinle-Neumann *et al.*, 2002), yielding a temperature of 4000 K at the core–mantle boundary. The influence of the light element on the Grüneisen parameter is not necessarily negligible and will need to be measured to test this prediction.

One of the most remarkable discoveries of core structure in recent years has been that of inner-core anisotropy. Longitudinal waves travel a few percent faster along a near polar axis than in the equatorial plane (Morelli *et al.*, 1986; Woodhouse *et al.*, 1986). Lattice-preferred orientation seems a natural explanation because all plausible crystalline phases of iron have single-crystal elastic anisotropy at the relevant conditions that exceeds that of the inner core (Stixrude and Cohen, 1995; Söderlind *et al.*, 1996), notwithstanding disagreements about the values of the high-temperature elastic constants as predicted by different approximate theories (Gannarelli *et al.*, 2005; Steinle-Neumann *et al.*, 2001). The identity of the stable phase is critical since the pattern of anisotropy in body-centered cubic and hexagonal candidates are very different. Although the body-centered cubic phase appears to be elastically unstable for pure iron, favoring a hexagonal close-packed inner core, there is some evidence that light elements and nickel tend to stabilize this structure (Lin *et al.*, 2002a; Lin *et al.*, 2002b; Vocadlo *et al.*, 2003). Still unknown is the source of stress that might produce preferred orientation, or knowledge of the dominant slip planes and critical resolved shear stresses that would permit prediction of texture given an applied stress. Further seismological investigations have shown that the structure of the inner core is also laterally heterogeneous (Creager, 1997; Su and Dziewonski, 1995; Tanaka and Hamaguchi, 1997), and that there may be a distinct innermost layer (Ishii and Dziewonski, 2002), which may be due to a phase transformation.

2.02.3 Lateral Heterogeneity

2.02.3.1 Overview

Lateral variations in seismic wave velocities have three sources: lateral variations in temperature, chemical composition, and phase assemblage (**Figure 10**). The first of these has received most attention. Indeed, comparison of tomographic models with surface tectonic features indicates that temperature may be the largest source of lateral variations: arcs are slow, cratons and subducting slabs are fast, and there is a good correlation between the history of past subduction and the location of fast velocity anomalies throughout the mantle. Quantifying these interpretations has proved challenging. One reason is that temperature is almost certainly not the only important factor. For example, it is recognized that continental mantle lithosphere must be depleted in order to remain dynamically stable, and that this depletion contributes along with temperature, to the velocity anomaly (Jordan, 1975). Throughout the upper 1000 km of the mantle, lateral variations in phase assemblage may contribute as much as the influence of temperature alone. In the lower mantle, it can be demonstrated that sources other than temperature are required to explain the lateral heterogeneity.

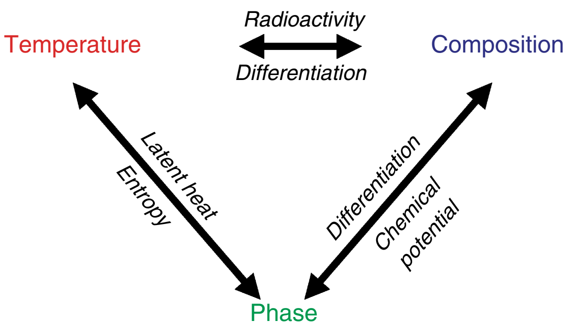

Figure 10 The three sources of lateral heterogeneity in Earth's mantle: lateral variations in temperature, in chemical composition, and phase. Arrows indicate that these three sources may influence each other. Increasing temperature alters the relative stability of phases via contrasts in entropy, and may generate changes in composition via differentiation caused by partial melting. Changes in composition may include changes in the concentration of radioactive heat producing elements and therefore temperature, and influence phase stability through the chemical potential. Changes in phase release or absorb latent heat, thus altering the temperature and may produce density contrasts that lead to differentiation, potentially altering the composition.

2.02.3.2 Temperature

Several studies have sought to estimate lateral variations in temperature in the upper mantle on the basis of tomographic models and measured properties of minerals (Godey *et al.*, 2004; Goes *et al.*, 2000; Sobolev *et al.*, 1996). These estimates are consistent with the results of geothermobarometry, surface tectonics, and heat flow observations. In one sense, the upper mantle is an ideal testing ground for the physical interpretation of mantle tomography because the elastic constants of the constituent minerals are relatively well known. But the upper mantle is also remarkably complex. A potentially important factor that is not accounted for in these studies is the lateral variations in phase proportions. Another source of uncertainty is anelasticity, which magnifies the temperature dependence of the velocity by an amount that is poorly constrained experimentally.

The temperature dependence of the seismic wave velocities of mantle minerals decreases rapidly with increasing pressure (**Figure 11**). If we ascribe a purely thermal origin to lateral structure, we would then expect the amplitude of tomographic models to decrease rapidly with depth. But tomographic models show a different pattern. The amplitude tends to decrease rapidly in the upper boundary layer, reaches a minimum at mid-mantle depths, and then increases with depth in the bottom half of the mantle. Part of the increase in amplitude with depth may be associated with the lower thermal boundary layer, where we would expect lateral temperature variations to exceed that in the mid-mantle. While concerns regarding radial resolution of tomographic models cannot be dismissed, it seems likely that this aspect of lower mantle structure cannot be explained by temperature alone.

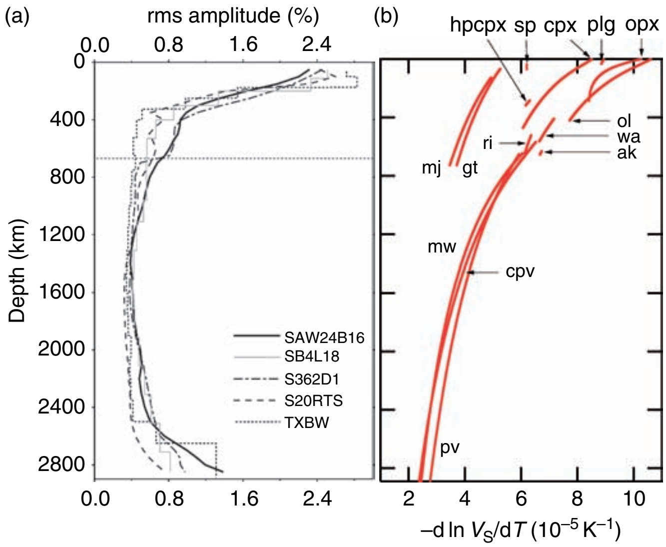

Figure 11 The amplitude of tomographic models as a function of depth (a) from (Romanowicz, 2003) as compared with the temperature derivative of the shear-wave velocity for mantle minerals along a typical isentrope (b) from (Stixrude and Lithgow-Bertelloni, 2005b).

Another indication that temperature alone cannot explain lower mantle structure is the comparison of lateral variations in S- and P-wave velocities. The ratio

$$R = \left(\frac{\delta \ln V_S}{\delta \ln V_P}\right)_z \qquad [10]$$

where V_S is the shear-wave speed and V_P is the longitudinal-wave speed and the subscript z indicates that variations are at constant depth, reaches values as large as 3.5 in the lower mantle and appears to increase systematically with increasing depth (Masters *et al.*, 2000; Ritsema and van Heijst, 2002; Robertson and Woodhouse, 1996). This is to be compared with

$$R_{\text{thermal}} = \left[\frac{(1-A)(\delta_S - 1)}{\Gamma - 1} + A\right]^{-1} \qquad [11]$$

where $A = 4/3V_S^2/V_P^2$, $\delta_S = (\partial \ln K_S/\partial \ln \rho)_P$, $\Gamma = (\partial \ln G/\partial \ln \rho)_P$. The ratio takes on its limiting value $R_{\text{thermal}} \rightarrow A^{-1} \approx 2.5$ as $\delta_S \rightarrow 1$. In some portions of the mantle, lateral variations in shear and bulk sound velocities appear to be anticorrelated: regions that are slow in V_S are fast in V_B (Masters *et al.*, 2000; Su and Dziewonski, 1997; Vasco and Johnson, 1998). Large values of R and anticorrelated V_S and V_B both require $\delta_S < 1$ if they are to be explained by temperature alone, a condition not met by lower mantle minerals. Lower mantle phases all have $\delta_S > 1$ so that longitudinal, shear, and bulk sound velocities all decrease with increasing temperature (Agnon and Bukowinski, 1990; Karki *et al.*, 1999; Oganov *et al.*, 2001; Wentzcovitch *et al.*, 2004). Anelasticity increases the value of R_{thermal} (Karato, 1993), but apparently not sufficiently to account for the tomographic value (Masters *et al.*, 2000), and in any case cannot produce anticorrelation in V_S and V_B.

2.02.3.3 Composition

Of the five major cations in the mantle, iron has the largest influence on the density and the elastic wave velocities. The influence of iron content on the shear velocity differs substantially among the major mantle minerals. This means that different bulk compositions (e.g., MORB, pyrolite) will have different sensitivities to lateral variations in iron content (**Figure 12**).

What sort of lateral variations in composition might explain the unusual features of lower mantle structure? A definitive answer is prevented by our ignorance of the elastic properties of lower mantle phases. Lateral variations in iron content do not appear capable of producing anticorrelation in bulk- and shear-wave velocity, as both velocities are decreased by addition of iron to $MgSiO_3$ perovskite (Kiefer *et al.*, 2002). It has been argued that lateral variations in Ca content can produce anticorrelation since $CaSiO_3$ perovskite has a greater shear-wave

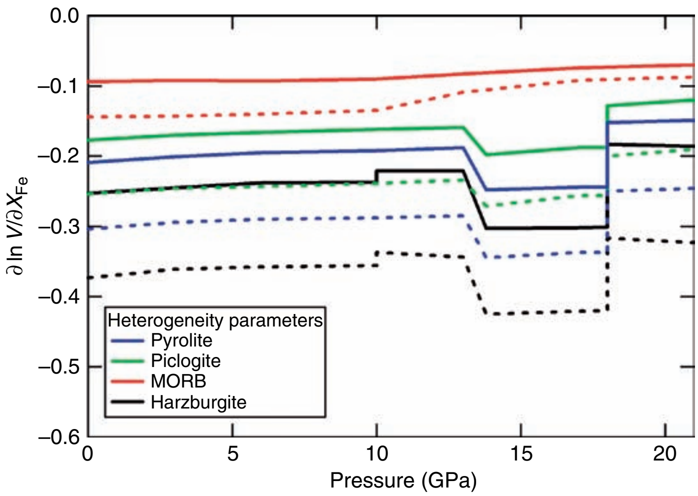

Figure 12 Sensitivity of compressional and shear-wave velocity heterogeneity parameters to Fe-Mg substitution calculated for pyrolite, piclogite, harzburgite, and MORB, along an isentropic pressure/temperature path with a potential temperature of 1673 K. Solid lines: $\partial \ln v_P/\partial X_{Fe}$, dashed lines: $\partial \ln v_S/\partial X_{Fe}$. From Speziale S, Fuming J, and Duffy TS (2005a) Compositional dependence of the elastic wave velocities of mantle minerals: Implications for seismic properties of mantle rocks. In: Matas J, van der Hilst RD, Bass JD, and Trampert J *Earth's Deep Mantle*: *Structure*, *Composition*, *and Evolution*, pp. 301–320. Washington, DC: American Geophysical Union.

velocity but lesser bulk sound velocity that $MgSiO_3$ perovskite (Karato and Karki, 2001). However, this argument is based on first-principles calculations of $CaSiO_3$ perovskite that assumed a cubic structure (Karki and Crain, 1998). One of the remarkable features of this phase is that it undergoes a slight noncubic distortion with decreasing temperature (Adams and Oganov, 2006; Ono *et al.*, 2004; Shim *et al.*, 2002; Stixrude *et al.*, 1996) that nevertheless produces a very large 15% softening of V_S, while leaving the density and V_B virtually unaffected (Stixrude *et al.*, 2007).

Dynamical models suggest that lateral variations in composition in the lower mantle may be associated with segregation of basalt (Christensen and Hofmann, 1994; Davies, 2006; Nakagawa and Buffett, 2005; Xie and Tackley, 2004). *In situ* equation of state studies indicate that basalt is denser than average mantle and would tend to pile up at the core–mantle boundary (Hirose *et al.*, 2005). Basalt-rich piles may be swept up by mantle convection, and may explain lower mantle anomalies with boundaries that are sharp, that is, of apparently nonthermal origin (Ni *et al.*, 2002), and primitive signatures in mantle geochemistry (Kellogg *et al.*, 1999). A definitive test of such scenarios awaits determination of the elastic properties of minerals in basalt that are currently unmeasured, such as a calcium-ferrite structured oxide.

2.02.3.4 Phase

The mantle is made of several different phases, with distinct elastic properties. As temperature varies, the relative proportions and compositions of these phases change, producing an additional contribution to laterally varying structure (**Figure 13**). This effect has been discussed in terms of thermally induced phase transformations (Anderson, 1987). The magnitude of the effect is

$$\left(\frac{\partial V}{\partial T}\right)_{P,\text{phase}} \approx f\left(\frac{\partial P}{\partial T}\right)_{\text{eq}}\frac{\Delta V}{\Delta P} \qquad [12]$$

where f is the volume fraction of the mantle composed of the transforming phases, ΔV is the velocity contrast between them, ΔP is the pressure range over which the transition occurs, and the derivative on the right-hand side is the effective Clapeyron slope. The effect is largest for sharp transitions, such as the olivine to wadsleyite transition, and in this case may also be described in terms of the topography of the transition. It is sensible to describe lateral variations in velocity due to phase equilibria in terms of topography when the topography exceeds the width of the phase transformation

$$\left(\frac{\partial P}{\partial T}\right)_{\text{eq}}\Delta T > \Delta P \qquad [13]$$

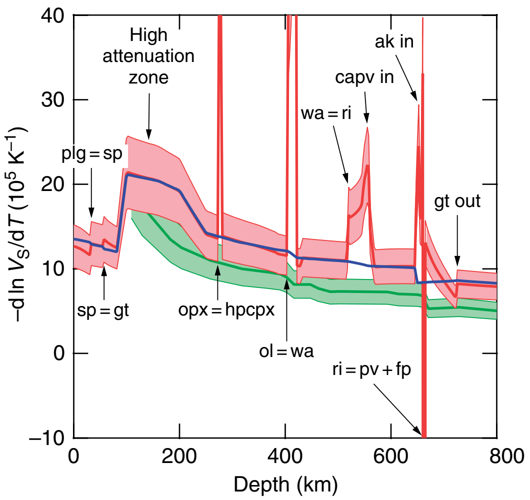

Figure 13 The variation of shear-wave velocity with temperature in pyrolite (red), including the effects of pressure, temperature, phase transformations, and anelasticity according to the model QR19 (Romanowicz, 1995) and $\alpha = 0.25$, and variation of Q with temperature given by $H^* = 430\,\mathrm{kJ\,mol^{-1}}$. The blue curve shows the derivative neglecting the influence of phase transformations. The green curve shows a similar calculation (Cammarano, *et al*., 2003) except that the effect of phase transformations is neglected. From Stixrude L and Lithgow-Bertelloni C (2007) Influence of phase transformations on lateral heterogeneity and dynamics in Earth's mantle. *Earth and Planetary Science Letters* (submitted).

where ΔT is the anticipated magnitude of lateral temperature variations. But the influence of phase transformations is also important for broad transitions such as pyroxene to garnet. In the upper mantle, most phase transitions have positive Clapeyron slopes. This means that, except in the vicinity of the 660 km discontinuity, phase transitions systematically increase the temperature dependence of seismic wave velocities throughout the upper 800 km of the mantle.

Lateral variations in phase have been invoked to explain some of the unusual features of the deep lower mantle, including the anticorrelation in bulk- and shear-wave velocities mentioned earlier (Iitaka *et al.*, 2004; Oganov and Ono, 2004; Tsuchiya *et al.*, 2004b; Wentzcovitch *et al.*, 2006). As perovskite transforms to postperovskite, the shear modulus increases while the bulk modulus decreases. Lateral variations in the relative abundance of these two phases caused, for example, by lateral variations in temperature, will then produce anticorrelated variations in V_S and V_B. Since the stability of the postperovskite phase is apparently restricted to the D″ layer, it is not clear whether this mechanism can explain all of the anomalous features of lower mantle tomography which appear to extend over a much greater depth interval. The high-spin to low-spin transition in iron may have a significant effect on the physical properties of ferropericlase and perovskite (Badro *et al.*, 2003, 2004; Cohen *et al.*, 1997; Li *et al.*, 2005; Pasternak *et al.*, 1997). Recent theoretical results indicate that the transition is spread out over hundreds of kilometers of depth and should affect laterally varying structure over much of the lower mantle (Tsuchiya *et al.*, 2006). The high-spin to low-spin transition increases the bulk modulus in ferropericlase (Lin *et al.*, 2005; Speziale *et al.*, 2005b). If it also increases the shear modulus, as Birch's law would predict, the transition would not account for anticorrelation of V_B and V_S.

2.02.4 Anisotropy

2.02.4.1 Overview

Anisotropy is a potentially powerful probe of mantle dynamics because it is produced by deformation. In dislocation creep, the easiest crystallographic slip plane tends to align with the plane of flow, and the easiest slip direction with the direction of flow. Since all mantle minerals are elastically anisotropic (**Figure 14**), this preferred orientation or texturing produces bulk anisotropy that is measurable by seismic waves. This mechanism for producing anisotropy is often referred to as lattice preferred orientation. Another mechanism is shape-preferred orientation in which the rheological contrast between the materials making up a composite cause them to be arranged inhomogeneously on deformation. Heterogeneous arrangements familiar from structural geology, including foliation and lineation, lead to anisotropy for seismic waves with wavelengths much longer than the scale length of heterogeneity.

Anisotropy is pervasive in the continental crust, and significant in the upper mantle, the D″ layer, and the inner core, the latter of which was discussed above in the section on the core. Anisotropy may also exist in the transition zone as indicated by global (Montagner and Kennett, 1996; Trampert and van Heijst, 2002) and regional (Fouch and Fischer, 1996) seismic models.

2.02.4.2 Upper Mantle

Anisotropy is well developed in the uppermost mantle. Studies of the seismic structure of this region, the

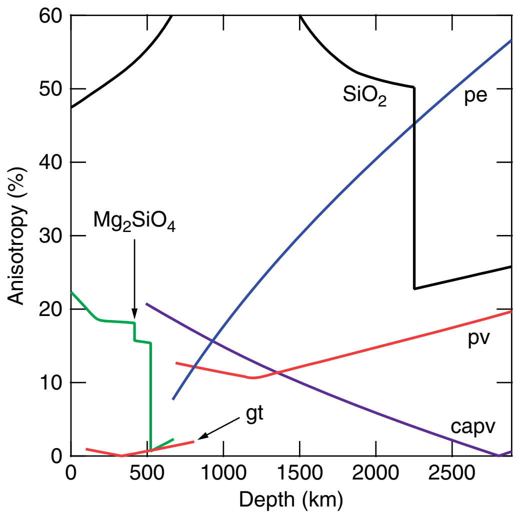

Figure 14 Single crystal azimuthal anisotropy of S-wave velocity in mantle minerals plotted, except for silica, over their pressure range of stability in pyrolite. The discontinuous changes in silica and Mg_2SiO_4 are due to phase transformations. The breaks in slope in garnet (pyrope), periclase, and calcium perovskite are due to interchanges in the fastest and slowest directions where the anisotropy passes through zero (Karki, *et al.*, 1997a). After Mainprice D, Barruol G, and Ismail WB (2000) The seismic anisotropy of the Earth's mantle: From single crystal to polycrystal. In: Karato SI, Forte A, Liebermann R, Masters G, and Stixrude L (eds.) *Earth's Deep Interior: Mineral Physics and Tomography from the Atomic to the Global Scale*. Washington, DC: American Geophysical Union.

texture of mantle samples, and the elastic properties of the constituent minerals have led to a simple first order picture. Convective flow in the upper mantle preferentially aligns olivine crystals such that the seismically fast direction is parallel to the flow direction (Christensen and Salisbury, 1979; Mainprice *et al.*, 2000). Two seismological signals are often distinguished, associated with different data sets and modeling strategies. Horizontally propagating shear waves travel at two different velocities depending on the direction of polarization: the faster is horizontal with V_{SH} and the slower is vertical with V_{SV}. The difference in velocity of the two polarizations is also referred to as shear-wave splitting. The shear-wave velocity also depends on the direction of propagation, and this is usually referred to as azimuthal anisotropy. Azimuthal anisotropy is also detected along vertically propagating paths via shear-wave splitting (Silver, 1996).

In detail, the picture of upper-mantle anisotropy is much richer than this first-order pattern. There are unexplained anomalies even in regions where the pattern of flow is presumably simple and large scale such as the Pacific basin. For example, the fast direction does not align everywhere with the direction of present-day plate motions (Montagner and Guillot, 2002; Tanimoto and Anderson, 1984). The magnitude of V_{SH}–V_{SV} varies spatially in a way that does not correlate simply with lithosphere age: the difference is maximum near the center of the north Pacific (Ekstrom and Dziewonski, 1998). At subduction zones, the fast direction is sometimes parallel, rather than normal to the trench (Fouch and Fischer, 1996; Russo and Silver, 1994). Explanations of these features will come from a better understanding of the development of texture in large-scale mantle flow (Chastel *et al.*, 1993; Ribe 1989), the preferred slip planes and critical resolved shear stresses in olivine and how these depend on stress, temperature, pressure, and impurities (Jung and Karato, 2001; Mainprice *et al.*, 2005), how stress and strain are partitioned between lithosphere and asthenosphere, and the relative importance of dislocation versus diffusion creep (Karato, 1992; van Hunen *et al.*, 2005).

2.02.4.3 D″ Layer

The D″ layer is also substantially anisotropic (Lay *et al.*, 1998b; Panning and Romanowicz, 2004). The minerals that make up this region all have large single-crystal anisotropies, with ferropericlase having the largest (Karki *et al.*, 2001; Stackhouse *et al.*, 2005; Wentzcovitch *et al.*, 2006) (**Figure 14**). The anisotropy of periclase depends strongly on pressure and actually reverses sense near 20 GPa: the directions of fastest and slowest elastic wave propagation interchange (Karki *et al.*, 1997a). This behavior emphasizes the importance of experimental measurements and first-principles predictions of elasticity at the relevant pressures. The easy glide planes of the minerals in D″ are unconstrained by experiment or first-principles theory. If one assumes that the easy glide planes are the same as those seen in ambient pressure experiments or analog materials, anisotropy produced by lattice preferred orientation in neither ferropericlase nor perovskite can explain the dominant pattern $V_{SH} > V_{SV}$ seen in seismology (Karato, 1998; Stixrude, 1998), while postperovskite does (Merkel *et al.*, 2006). One must be cautious, because the sense and magnitude of anisotropy depends strongly on the easy glide plane.

2.02.5 Attenuation and Dispersion

2.02.5.1 Overview

The Earth is not a perfectly elastic medium, even at seismic frequencies. There are two important consequences. Attenuation refers to the loss of amplitude of the elastic wave with propagation. Dispersion refers to the dependence of the elastic-wave velocity on the frequency. It can be shown that attenuation and dispersion are intimately related. Indeed, the importance of attenuation in the Earth first alerted seismologists to the dispersion that should yield a difference in velocities between low-frequency normal mode oscillations and higher-frequency body waves. The magnitude of attenuation is measured by the inverse quality factor Q^{-1}, the fractional energy loss per cycle.

From the mineralogical point of view, attenuation is potentially important as a very sensitive probe of temperature and minor element composition (Karato, 1993; Karato and Jung, 1998). Because attenuation is caused at the atomic scale by thermally activated processes, its magnitude is expected to depend exponentially on temperature. By analogy with the viscosity, the attenuation is expected also to depend strongly on the concentration of water, although there are as yet no experimental constraints on this effect. But with this promise come formidable challenges. Dissipative processes depend on defect concentrations and dynamics and/or the presence of multiple scales, such as grains and grain boundaries. These are much more challenging to study in the laboratory than equilibrium thermodynamic properties such as the elastic response.

2.02.5.2 Influence of Temperature

The most thorough study of attenuation is of olivine aggregates, specially fabricated to have approximately uniform grain size and minimal dislocation density (Gribb and Cooper, 1998; Jackson *et al.*, 2002). Whether such samples are representative of the mantle is an important question, although at this stage, when experimental data are so few, the need for precise and reproducible results is paramount. The key results of Jackson *et al.* (2002) within the seismic frequency band (~1–100 s) and in the limit of small attenuation, are consistent with the following relations:

$$Q^{-1}(P,T,\omega) = Ad^{-m}\omega^{-\alpha}\exp\left(-\alpha\frac{E^*+PV^*}{RT}\right) \quad [14]$$

$$V(P,T,\omega) = V(P,T,\infty)\times\left[1-\frac{1}{2}\cot\left(\frac{\alpha\pi}{2}\right)Q^{-1}(P,T,\omega)\right] \quad [15]$$

where ω is the frequency, d is the grain size, $m=0.28$ is the grain size exponent, $\alpha=0.26$, $E^*=430\ \mathrm{kJ\ mol^{-1}}$ is the activation energy, V^* is the activation volume, and R is the gas constant. For the experimental value of α, the factor multiplying Q^{-1} in eqn [15] has the value 1.16. The activation volume is currently unconstrained, which means the influence of pressure on attenuation is highly uncertain, although this quantity has been measured for other rheological properties such as viscosity and climb-controlled dislocation creep in olivine. Partial melt in the amount of 1% increases Q^{-1} by a factor that depends weakly on frequency and grain size and is approximately 2 in the seismic band and for plausible grain sizes (1–10 mm) (Faul *et al.*, 2004). The influence of crystallographically bound hydrogen on the attenuation is currently unconstrained, although it is known that the viscosity decreases with increasing hydrogen concentration (Mei and Kohlstedt, 2000a, 2000b). The second relation makes the relationship explicit between attenuation and dispersion. Equations [14] and [15] are consistent with earlier theories developed primarily on the basis of seismological observations and the idea of a distribution of dissipitave relaxation times in solids (Anderson, 1989).

An important consequence of eqn [15] is that, if the value of the frequency exponent is known, the magnitude of the dispersion depends only on the value of Q^{-1}. This means that it is possible directly to relate seismological velocity models to experimental measurements in the elastic limit. Knowing the seismological value of Q^{-1} and V, one may compute $V(\infty)$ and compare this directly with high-frequency experiments or first-principles calculations. Alternatively, one may correct elastic wave velocities according to the seismological value of Q^{-1} in order to compare with the seismological velocity model (Stixrude and Lithgow-Bertelloni, 2005a). These considerations are most important in the low velocity zone where $1000/Q$ reaches 20 and the difference in velocity between the elastic limit and the seismic band may be as great as 2%.

Attenuation enhances the temperature dependence of seismic wave velocities and is important to consider in the interpretation of seismic tomography (Karato, 1993). The temperature derivative of eqn [15] is

$$\frac{\partial \ln V(\omega)}{\partial T} = \frac{\partial \ln V(\infty)}{\partial T} - \frac{1}{2}\cot\left(\frac{\alpha\pi}{2}\right)Q^{-1}\frac{H^*}{RT^2} \quad [16]$$

where $H^* = E^* + PV^*$ is the activation enthalpy. For $\alpha = 0.26$, $H^* = 430\,\mathrm{kJ\,mol^{-1}}$, $1000/Q = 10$, and $T = 1600\,\mathrm{K}$, the second term is $-6 \times 10^{-5}\,\mathrm{K^{-1}}$, nearly as large as the elastic temperature derivative neglecting the influence of phase transformations (**Figure 11**).

Laboratory studies predict large lateral variations in attenuation in the mantle. Over a range of temperature 1500–1600 K, the attenuation varies by a factor of 2. This extreme sensitivity promises powerful constraints on the temperature structure of the mantle that are complimentary to those derived from the elastic wave speeds. Attenuation tomography reveals a decrease in Q^{-1} with increasing lithospheric age from 0–100 Ma in the Pacific low velocity zone of approximately one order of magnitude (Romanowicz, 1998). Arcs appear to have exceptionally high attenuation (Barazangi and Isacks, 1971; Roth *et al.*, 2000). Unraveling the relative contributions of partial melt, water concentration, and other factors (grain size?) to this observation will provide unique constraints on the process of arc magma generation. This program is still limited by the lack of experimental data on the influence of water content on Q.

2.02.5.3 Speculations on the Influence of Pressure

Comparisons of laboratory determinations to radial seismological models of Q^{-1} reveal some surprises. The comparison is hampered by the fact that there are currently no experimental data at elevated pressure. Two models have been explored in the literature, eqn [14] with the activation volume assumed to be independent of pressure and temperature, and the homologous temperature formulation in which activated properties are assumed to scale with the ratio of the absolute temperature to melting temperature (Weertman, 1970)

$$Q^{-1}(P,T,\omega) = Ad^{-m}\omega^{-\alpha}\exp\left[-\alpha\frac{gT_{\mathrm{m}}(P)}{T}\right] \qquad [17]$$

where $T_{\mathrm{m}}(P)$ is the melting temperature as a function of pressure, and the parameter g is assumed to be constant. Neither of these models resembles the variation of Q^{-1} in the vicinity of the low velocity zone (**Figure 15**). The high attenuation zone in the mantle is much more sharply defined at its lower boundary than either eqn [14] or [17]. While the limited vertical resolution of the seismological Q models cannot be overlooked, the comparison seems to imply either (1) eqns [14] and [17] do not represent the pressure

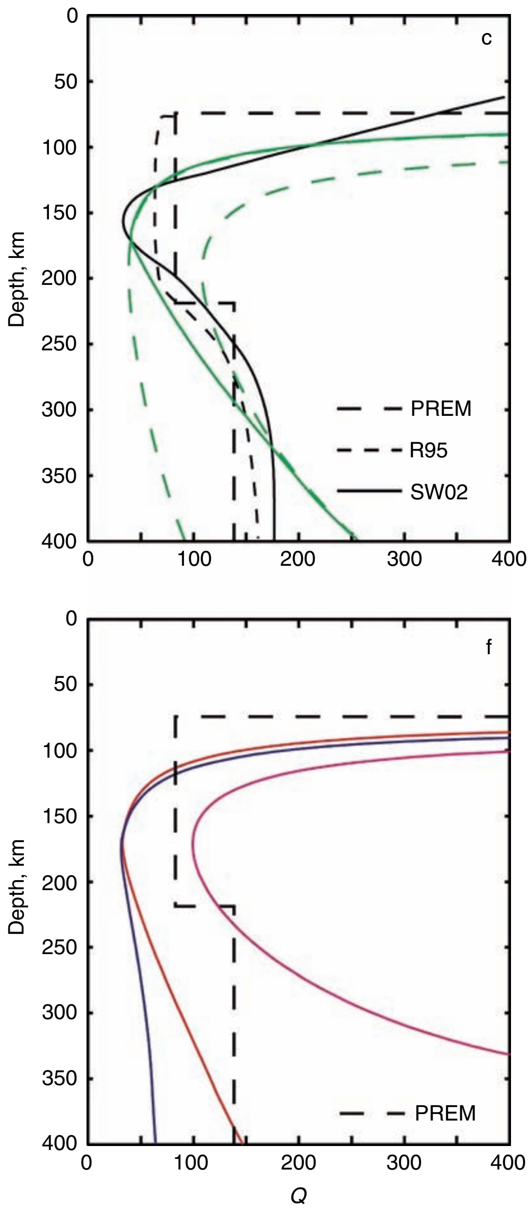

Figure 15 Quality profiles calculated assuming a range of temperatures and activation volumes and grain size either independent of depth (dashed curves in upper figure, rightmost pink curve in lower figure), or increasing by a factor of 5 (solid curve in upper figure) or 2 (red and blue curves in lower figure) as a function of depth, compared with seismological attenuation models (Dziewonski and Anderson, 1981; Romanowicz, 1995; Selby and Woodhouse, 2002). From Faul UH and Jackson I (2005) The seismological signature of temperature and grain size variations in the upper mantle. *Earth and Planetary Science Letters* 234: 119–134.

dependence of activated processes, at least not those responsible for dissipation in the seismic band in the mantle; (2) there is a change in the composition or phase of the mantle at this depth, for example, a change in water content or partial melt fraction; (3) there is a change in the physical mechanism of attenuation at the base of the low velocity zone. Faul and Jackson (2005) have proposed that the base of the low velocity zone represents a rapid change in grain size with increasing depth, although the mechanism by which such a change could occur is uncertain.

2.02.6 Conclusions

Over the past decade, studies of the seismic properties of major earth forming materials have dramatically expanded in scope. The field has moved from measurements of the elastic properties of individual minerals at elevated pressure and temperature to now include studies of deformation mechanisms and their relationship to the development of anisotropy, attenuation, and dispersion, and the interplay between phase equilibria and elasticity in mantle assemblages approaching realistic bulk compositions. Major challenges remain in each of the mantle's regions. Upper-mantle structure is remarkably rich and surprisingly full of features that resist explanation, such as the discontinuity structure and the high velocity gradient. Phase transformations are ubiquitous in the transition zone: there is no depth at which a transformation is not in progress, so that understanding this region will require the continued development of thermodynamic models of the mantle that are simultaneously able to capture phase equilibria and physical properties. The lower mantle still lies beyond the reach of many experimental techniques for measuring the elastic constants and most of our knowledge of elasticity in this region comes from first-principles theory. New physics in the lower mantle, including high-spin to low-spin transitions, the postperovskite transition, and valence state changes, promise new solutions to problems such as the anticorrelation between bulk- and shear-wave velocity variations, and fertile ground for new ideas. Many classic problems of the core, including its composition and temperature, seem to be yielding to new approaches and promise new constraints on the origin and evolution of Earth's deepest layer. At the same time, the seismic structure of the inner core, including its anisotropy, heterogeneity, and layering, remains enigmatic.

References

Adams DJ and Oganov AR (2006) *Ab initio* molecular dynamics study of $CaSiO_3$ perovskite at P–T conditions of Earth's lower mantle. *Physical Review B* 73: 184106.

Agnon A and Bukowinski MST (1990) Delta s at high-pressure and dlnvs/dlnvp in the lower mantle. *Geophysical Research Letters* 17: 1149–1152.

Akaogi M, Ito E, and Navrotsky A (1989) Olivine-modified spinel–spinel transitions in the system Mg_2SiO_4–Fe_2SiO_4 – Calorimetric measurements, thermochemical calculation, and geophysical application. *Journal of Geophysical Research, Solid Earth and Planets* 94: 15671–15685.

Akaogi M, Tanaka A, and Ito E (2002) Garnet–ilmenite–perovskite transitions in the system $Mg_4Si_4O_{12}$–$Mg_3Al_2Si_3O_{12}$ at high pressures and high temperatures: Phase equilibria, calorimetry and implications for mantle structure. *Physics of the Earth and Planetary Interiors* 132: 303–324.

Alfe D, Gillan MJ, and Price GD (2002a) Composition and temperature of the Earth's core constrained by combining *ab initio* calculations and seismic data. *Earth and Planetary Science Letters* 195: 91–98.

Alfe D, Price GD, and Gillan MJ (2002b) Iron under Earth's core conditions: Liquid-state thermodynamics and high-pressure melting curve from *ab initio* calculations. *Physical Review B* 65: 165118.

Anderson DL (1987) Thermally induced phase-changes, lateral heterogeneity of the mantle, continental roots, and deep slab anomalies. *Journal of Geophysical Research, Solid Earth and Planets* 92: 13968–13980.

Anderson DL (1989) *Theory of the Earth*, 366pp. Boston: Blackwell Scientific.

Anderson DL and Sammis C (1969) The low velocity zone. *Geofisica Internacional* 9: 3–19.

Anderson OL (1995) *Equations of State of Solids for Geophysics and Ceramic Science*. Oxford: Oxford University Press.

Anderson OL and Isaak DG (2002) Another look at the core density deficit of Earth's outer core. *Physics of the Earth and Planetary Interiors* 131: 19–27.

Anderson OL, Schreiber E, Liebermann RC, and Soge N (1968) Some elastic constant data on minerals relevant to geophysics. *Reviews of Geophysics* 6: 491–524.

Angel RJ, Chopelas A, and Ross NL (1992) Stability of high-density clinoenstatite at upper-mantle pressures. *Nature* 358: 322–324.

Badro J, Fiquet G, Guyot F, *et al.* (2003) Iron partitioning in Earth's mantle: Toward a deep lower mantle discontinuity. *Science* 300: 789–791.

Badro J, Rueff J-P, Vankó G, Monaco G, Fiquet G, and Guyot F (2004) Electronic transitions in perovskite: Possible nonconvecting layers in the lower mantle. *Science* 305: 383–386.

Barazangi M and Isacks B (1971) Lateral variations of seismic-wave attenuation in upper mantle above inclined earthquake zone of Tonga Island Arc – Deep anomaly in upper mantle. *Journal of Geophysical Research* 76: 8493–8515.

Benz HM and Vidale JE (1993) Sharpness of upper-mantle discontinuities determined from high-frequency reflections. *Nature* 365: 147–150.

Bercovici D and Karato S (2003) Whole-mantle convection and the transition-zone water filter. *Nature* 425: 39–44.

Birch F (1964) Density and composition of the mantle and core. *Journal of Geophysical Research* 69: 4377–4388.

Birch F (1969) Density and compostion of the upper mantle: First approximation as an olivine layer. In: Hart PJ (ed.) *The Earth's Crust and Upper Mantle*, pp. 18–36. Washington, DC: American Geophysical Union.

Bostock MG (1998) Mantle stratigraphy and evolution of the slave province. *Journal of Geophysical Research, Solid Earth* 103: 21183–21200.

Brown JM and McQueen RG (1982) The equation of state for iron and the Earth's core. In: Akimoto S and Manghnani MH (eds.) *High Pressure Research in Geophysics*, pp. 611–623. Dordrecth: Reidel.

Brown JM and McQueen RG (1986) Phase transitions, Grüneisen parameter, and elasticity for shocked iron between 77 GPa and 400 GPa. *Journal of Geophysical Research* 91: 7485–7494.

Brown JM and Shankland TJ (1981) Thermodynamic parameters in the Earth as determined from seismic profiles. *Geophysical Journal of the Royal Astronomical Society* 66: 579–596.

Buffett BA, Garnero EJ, and Jeanloz R (2000) Sediments at the top of Earth's core. *Science* 290: 1338–1342.

Cammarano F, Saskia G, Pierre V, and Domenico G (2003) Inferring upper-mantle temperatures from seismic velocities. *Physics of the Earth and Planetary Interiors* 138: 197–222.

Carpenter MA, Hemley RJ, and Ho-kwang M (2000) High-pressure elasticity of stishovite and the P4(2)/mnm reversible arrow Pnnm phase transition. *Journal of Geophysical Research, Solid Earth* 105: 10807–10816.

Castle JC and van der Hilst RD (2003) Searching for seismic scattering off mantle interfaces between 800 km and 2000 km depth. *Journal of Geophysical Research, Solid Earth* 108: 2095.

Chastel YB, Dawson PR, Wenk H-R, and Bennett K (1993) Anisotropic convection with implications for the upper-mantle. *Journal of Geophysical Research, Solid Earth* 98: 17757–17771.

Christensen UR and Hofmann AW (1994) Segregation of subducted oceanic-crust in the convecting mantle. *Journal of Geophysical Research, Solid Earth* 99: 19867–19884.

Christensen NI and Salisbury MH (1979) Seismic anisotropy in the upper mantle: Evidence from the Bay of Islands ophiolite complex. *Journal of Geophysical Research* 84: 4601–4610.

Christensen UR and Yuen DA (1985) Layered convection induced by phase transitions. *Journal of Geophysical Research* 90: 10291–10300.

Chudinovskikh L and Boehler R (2001) High-pressure polymorphs of olivine and the 660-km seismic discontinuity. *Nature* 411: 574–577.

Cohen RE, Mazin II, and Isaak DG (1997) Magnetic collapse in transition metal oxides at high pressure: Implications for the Earth. *Science* 275: 654–657.

Creager KC (1997) Inner core rotation rate from small-scale heterogeneity and time-varying travel times. *Science* 278: 1284–1288.

Davies GF (2006) Gravitational depletion of the early Earth's upper mantle and the viability of early plate tectonics. *Earth and Planetary Science Letters* 243: 376–382.

Deuss A and Woodhouse JH (2001) Seismic observations of splitting of the mid-transition zone discontinuity in Earth's mantle. *Science* 294: 354–357.

Deuss A and Woodhouse JH (2002) A systematic search for mantle discontinuities using SS-precursors. *Geophysical Research Letters* 29: doi:10.1029/2002GL014768.

Deuss A, Redfern SAT, Chambers K, and Woodhouse JH (2006) The nature of the 660-kilometer discontinuity in Earth's mantle from global seismic observations of PP precursors. *Science* 311: 198–201.

Dobson DP and Brodholt JP (2005) Subducted banded iron formations as a source of ultralow-velocity zones at the core–mantle boundary. *Nature* 434: 371–374.

Duffy TS, Zha C-S, Downs RT, Ho-kwang M, and Russell JH (1995) Elasticity of forsterite to 16 GPa and the composition of the upper-mantle. *Nature* 378: 170–173.

Dziewonski AM and Anderson DL (1981) Preliminary reference earth model. *Physics of the Earth and Planetary Interiors* 25: 297–356.

Ekstrom G and Dziewonski AM (1998) The unique anisotropy of the Pacific upper mantle. *Nature* 394: 168–172.

Faul UH, Fitz Gerald JD, and Jackson I (2004) Shear wave attenuation and dispersion in melt-bearing olivine polycrystals: 2. Microstructural interpretation and seismological implications. *Journal of Geophysical Research, Solid Earth* 109: B06202 (doi:10.1029/2003JB002407).

Faul UH and Jackson I (2005) The seismological signature of temperature and grain size variations in the upper mantle. *Earth and Planetary Science Letters* 234: 119–134.

Fei Y, Ho-Kwang M, and Mysen BO (1991) Experimental-determination of element partitioning and calculation of phase-relations in the MgO–FeO–SiO_2 system at high-pressure and high-temperature. *Journal of Geophysical Research, Solid Earth and Planets* 96: 2157–2169.

Fei Y, Van Orman J, Li J, *et al.* (2004) Experimentally determined postspinel transformation boundary in Mg_2SiO_4 using MgO as an internal pressure standard and its geophysical implications. *Journal of Geophysical Research, Solid Earth* 109: B02305 (doi:10.1029/2003JB002562).

Flanagan MP and Shearer PM (1998) Global mapping of topography on transition zone velocity discontinuities by stacking SS precursors. *Journal of Geophysical Research, Solid Earth* 103: 2673–2692.

Fouch MJ and Fischer KM (1996) Mantle anisotropy beneath northwest Pacific subduction zones. *Journal of Geophysical Research, Solid Earth* 101: 15987–16002.

Frost DJ (2003) The structure and sharpness of $(Mg, Fe)_2SiO_4$ phase transformations in the transition zone. *Earth and Planetary Science Letters* 216: 313–328.

Fujisawa H (1998) Elastic wave velocities of forsterite and its beta-spinel form and chemical boundary hypothesis for the 410-km discontinuity. *Journal of Geophysical Research, Solid Earth* 103: 9591–9608.

Gaherty JB and Jordan TH (1995) Lehmann discontinuity as the base of an anisotropic layer beneath continents. *Science* 268: 1468–1471.

Gaherty JB, Kato M, and Jordan TH (1999a) Seismological structure of the upper mantle: A regional comparison of seismic layering. *Physics of the Earth and Planetary Interiors* 110: 21–41.

Gaherty JB, Yanbin W, Jordan TH, and Weidner DJ (1999b) Testing plausible upper-mantle compositions using fine-scale models of the 410-km discontinuity. *Geophysical Research Letters* 26: 1641–1644.

Gannarelli CMS, Alfe D, and Gillan MJ (2005) The axial ratio of hcp iron at the conditions of the Earth's inner core. *Physics of the Earth and Planetary Interiors* 152: 67–77.

Garnero EJ and Helmberger DV (1996) Seismic detection of a thin laterally varying boundary layer at the base of the mantle beneath the central-Pacific. *Geophysical Research Letters* 23: 977–980.

Garnero EJ and Jeanloz R (2000) Fuzzy patches on the Earth's core–mantle boundary? *Geophysical Research Letters* 27: 2777–2780.

Godey S, Deschamps F, Trampert J, and Snieder R (2004) Thermal and compositional anomalies beneath the North American continent. *Journal of Geophysical Research, Solid Earth* 109: B01308 (doi:10.1029/2002JB002263).

Goes S, Govers R, and Vacher P (2000) Shallow mantle temperatures under Europe from P and S wave tomography. *Journal of Geophysical Research, Solid Earth* 105: 11153–11169.

Gossler J and Kind R (1996) Seismic evidence for very deep roots of continents. *Earth and Planetary Science Letters* 138: 1–13.

Grand SP and Helmberger DV (1984) Upper mantle shear structure of North-America. *Geophysical Journal of the Royal Astronomical Society* 76: 399–438.

Graves RW and Helmberger DV (1988) Upper mantle cross-section from Tonga to Newfoundland. *Journal of Geophysical Research, Solid Earth and Planets* 93: 4701–4711.

Green DH and Liebermann RC (1976) Phase-equilibria and elastic properties of a pyrolite model for oceanic upper mantle. *Tectonophysics* 32: 61–92.

Gribb TT and Cooper RF (1998) Low-frequency shear attenuation in polycrystalline olivine: Grain boundary diffusion and the physical significance of the Andrade model for viscoelastic rheology. *Journal of Geophysical Research, Solid Earth* 103: 27267–27279.

Gu Y, Dziewonski AM, and Agee CB (1998) Global de-correlation of the topography of transition zone discontinuities. *Earth and Planetary Science Letters* 157: 57–67.

Gu YJ, Dziewonski AM, and Ekström G (2001) Preferential detection of the Lehmann discontinuity beneath continents. *Geophysical Research Letters* 28: 4655–4658.

Gung YC, Panning M, and Bomanowicz B (2003) Global anisotropy and the thickness of continents. *Nature* 422: 707–711.

Gutenberg B (1959) Wave velocities below the mohorovicic discontinuity. *Geophysical Journal of the Royal Astronomical Society* 2: 348–352.

Gwanmesia GD, Rigden S, Jackson I, and Liebermann RC (1990) Pressure-dependence of elastic wave velocity for beta-Mg_2SiO_4 and the composition of the Earths mantle. *Science* 250: 794–797.

Helffrich G (2000) Topography of the transition zone seismic discontinuities. *Reviews of Geophysics* 38: 141–158.

Helffrich G and Bina CR (1994) Frequency-dependence of the visibility and depths of mantle seismic discontinuities. *Geophysical Research Letters* 21: 2613–2616.

Helffrich GR and Wood BJ (1996) 410 km discontinuity sharpness and the form of the olivine alpha–beta phase diagram: Resolution of apparent seismic contradictions. *Geophysical Journal International* 126: F7–F12.

Hirose K (2002) Phase transitions in pyrolitic mantle around 670-km depth: Implications for upwelling of plumes from the lower mantle. *Journal of Geophysical Research, Solid Earth* 107: B42078 (doi:10.1029/2001JB000597).

Hirose K, Komabayashi T, Murakami M, and Funakoshi K-i (2001) *In situ* measurements of the majorite–akimotoite–perovskite phase transition boundaries in $MgSiO_3$. *Geophysical Research Letters* 28: 4351–4354.

Hirose K, Takafuji N, Sata N, and Ohishi Y (2005) Phase transition and density of subducted MORB crust in the lower mantle. *Earth and Planetary Science Letters* 237: 239–251.

Hirschmann MM, Abaud C, and Withers AC (2005) Storage capacity of H_2O in nominally anhydrous minerals in the upper mantle. *Earth and Planetary Science Letters* 236: 167–181.

Iitaka T, Hirose K, Kawamura K, and Murakami M (2004) The elasticity of the $MgSiO_3$ post-perovskite phase in the Earth's lowermost mantle. *Nature* 430: 442–445.

Irifune T and Isshiki M (1998) Iron partitioning in a pyrolite mantle and the nature of the 410-km seismic discontinuity. *Nature* 392: 702–705.

Irifune T, Nishiyama N, Kuroda K, *et al.* (1998) The postspinel phase boundary in Mg_2SiO_4 determined by *in situ* X-ray diffraction. *Science* 279: 1698–1700.

Ishii M and Dziewonski AM (2002) The innermost inner core of the Earth: Evidence for a change in anisotropic behavior at the radius of about 300 km. *Proceedings of the National Academy of Sciences of the United States of America* 99: 14026–14030.

Ita J and Stixrude L (1992) Petrology, elasticity, and composition of the mantle transition zone. *Journal of Geophysical Research, Solid Earth* 97: 6849–6866.

Ito E and Takahashi E (1989) Postspinel transformations in the system Mg_2SiO_4–Fe_2SiO_4 and some geophysical implications. *Journal of Geophysical Research, Solid Earth and Planets* 94: 10637–10646.

Jackson I, *et al.* (2002) Grain-size-sensitive seismic wave attenuation in polycrystalline olivine. *Journal of Geophysical Research, Solid Earth* 107: B122360 (doi:10.1029/2001JB001225).

Jaupart C and Mareschal JC (1999) The thermal structure and thickness of continental roots. *Lithos* 48: 93–114.

Jeanloz R and Thompson AB (1983) Phase transitions and mantle discontinuities. *Reviews of Geophysics* 21: 51–74.

Johnson LR (1969) Array measurements of P velocities in lower mantle. *Bulletin of the Seismological Society of America* 59: 973–1008.

Jordan TH (1975) Continental tectosphere. *Reviews of Geophysics* 13: 1–12.

Jung H and Karato S (2001) Water-induced fabric transitions in olivine. *Science* 293: 1460–1463.

Kaneshima S and Helffrich G (1998) Detection of lower mantle scatterers northeast of the Marianna subduction zone using short-period array data. *Journal of Geophysical Research, Solid Earth* 103: 4825–4838.

Karato S (1992) On the Lehmann discontinuity. *Geophysical Research Letters* 19: 2255–2258.

Karato S (1993) Importance of anelasticity in the interpretation of seismic tomography. *Geophysical Research Letters* 20: 1623–1626.

Karato S and Jung H (1998) Water, partial melting and the origin of the seismic low velocity and high attenuation zone in the upper mantle. *Earth and Planetary Science Letters* 157: 193–207.

Karato S and Karki BB (2001) Origin of lateral variation of seismic wave velocities and density in the deep mantle. *Journal of Geophysical Research, Solid Earth* 106: 21771–21783.

Karato S-I (1998) Seismic anisotropy in the deep mantle, boundary layers and the geometry of mantle convection. *Pure and Applied Geophysics* 151: 565–587.

Karki BB and Crain J (1998) First-principles determination of elastic properties of $CaSiO_3$ perovskite at lower mantle pressures. *Geophysical Research Letters* 25: 2741–2744.

Karki BB and Stixrude L (1999) Seismic velocities of major silicate and oxide phases of the lower mantle. *Journal of Geophysical Research* 104: 13025–13033.

Karki BB, Stixrude L, Clark SJ, Warren MC, Ackland GJ, and Crain J (1997a) Structure and elasticity of MgO at high pressure. *American Mineralogist* 82: 51–60.

Karki BB, Stixrude L, and Crain J (1997b) *Ab initio* elasticity of three high-pressure polymorphs of silica. *Geophysical Research Letters* 24: 3269–3272.

Karki BB, Stixrude L, and Wentzcovitch RM (2001) High-pressure elastic properties of major materials of Earth's mantle from first principles. *Reviews of Geophysics* 39: 507–534.

Karki BB, Wentzcovitch RM, de Gironcoli S, and Baroni S (1999) First-principles determination of elastic anisotropy and wave velocities of MgO at lower mantle conditions. *Science* 286: 1705–1707.

Katsura T and Ito E (1989) The system Mg_2SiO_4–Fe_2SiO_4 at high-pressures and temperatures – Precise determination of stabilities of olivine, modified spinel, and spinel. *Journal of Geophysical Research, Solid Earth and Planets* 94: 15663–15670.

Katsura T, Yamada H, Nishikawa O, *et al.* (2004) Olivine–wadsleyite transition in the system $(Mg, Fe)_2SiO_4$. *Journal of

Geophysical Research, Solid Earth 109: B02209 (doi:10.1029/2003JB002438).

Kawakatsu H and Niu FL (1994) Seismic evidence for a 920-km discontinuity in the mantle. *Nature* 371: 301–305.

Kellogg LH, Hager BH, and van der Hilst RD (1999) Compositional stratification in the deep mantle. *Science* 283: 1881–1884.

Kennett BLN (1993) Seismic structure and heterogeneity in the upper mantle. In: Aki K and Dmowska R (eds.) *Relating Geophysics Structures and Processes: The Jeffreys Volume; Geophysical Monograph 76*. Washington, DC: American Geophysical Union and International Union of Geodosy and Geophysics.

Kennett BLN and Engdahl ER (1991) Traveltimes for global earthquake location and phase identification. *Geophysical Journal International* 105: 429–465.

Kiefer B, Stixrude L, and Wentzcovitch RM (2002) Elasticity of (Mg, Fe)SiO_3–Perovskite at high pressures. *Geophysical Research Letters* 29: 1539 (doi:10.1029/2002GL014683).

Klein EM and Langmuir CH (1987) Global correlations of ocean ridge basalt chemistry with axial depth and crustal thickness. *Journal of Geophysical Research, Solid Earth and Planets* 92: 8089–8115.

Knittle E and Jeanloz R (1989) Simulating the core-mantle boundary; an experimental study of high-pressure reactions between silicates and liquid iron. *Geophysical Research Letters* 16: 609–612.

Koito S, Akaogi M, Kubota O, and Suzuki T (2000) Calorimetric measurements of perovskites in the system $CaTiO_3$–$CaSiO_3$ and experimental and calculated phase equilibria for high-pressure dissociation of diopside. *Physics of the Earth and Planetary Interiors* 120: 1–10.

Kung J, Li B, Uchida T, and Wang Y (2005) *In situ* elasticity measurement for the unquenchable high-pressure clinopyroxene phase: Implication for the upper mantle. *Geophysical Research Letters* 32: L01307 (doi:10.1029/2004GL021661).

Lambert IB and Wyllie PJ (1968) Stability of hornblende and a model for low velocity zone. *Nature* 219: 1240–1241.

Lay T and Helmberger DV (1983) A lower mantle s-wave triplication and the shear velocity structure of D″. *Geophysical Journal of the Royal Astronomical Society* 75: 799–837.

Lay T, Williams Q, and Garnero EJ (1998a) The core–mantle boundary layer and deep Earth dynamics. *Nature* 392: 461–468.

Lay T, Garnero EJ, William Q, *et al.* (1998b) Seismic wave anisotropy in the D″ region and its implications. In: Gurnis M, Wysession ME, Knittle E, and Buffett BA (eds.) *The Core–Mantle Boundary Region*, pp. 299–318. Washington, DC: American Geophysical Union.

Lees AC, Bukowinski MST, and Jeanloz R (1983) Reflection properties of phase-transition and compositional change models of the 670-km discontinuity. *Journal of Geophysical Research* 88: 8145–8159.

Lestunff Y, Wicks CW, Jr., and Romanowicz B (1995) P'P' precursors under Africa – Evidence for mid-mantle reflectors. *Science* 270: 74–77.

Li B, Liebermann RC, and Weidner DJ (1998) Elastic moduli of wadsleyite (beta-Mg_2SiO_4) to 7 gigapascals and 873 Kelvin. *Science* 281: 675–677.

Li J and Agee CB (1996) Geochemistry of mantle–core differentiation at high pressure. *Nature* 381: 686–689.

Li L, Brodholt JP, Stackhouse S, Weidner DJ, Alfredsson M, and Price GD (2005) Electronic spin state of ferric iron in Al-bearing perovskite in the lower mantle. *Geophysical Research Letters* 32: L17307 (doi:10.1029/2005GL023045).

Lin JF, Heinz DL, Campbell AJ, Devine JM, Mao WL, and Shen G (2002a) Iron–nickel alloy in the Earth's core. *Geophysical Research Letters* 29: 1471 (doi:10.1029/2002GL015089).

Lin JF, Heinz DL, Campbell AJ, Devine JM, and Shen G (2002b) Iron–silicon alloy in Earth's core? *Science* 295: 313–315.

Lin JF, Struzhkin VV, Jacobsen SD, *et al.* (2005) Spin transition of iron in magnesiowustite in the Earth's lower mantle. *Nature* 436: 377–380.

Litasov K, Ohtani E, Suzuki A, and Funakoshi K (2005) *In situ* X-ray diffraction study of post-spinel transformation in a peridotite mantle: Implication for the 660-km discontinuity. *Earth and Planetary Science Letters* 238: 311–328.

Liu J, Chen G, Gwanmesia GD, and Liebermann RC (2000) Elastic wave velocities of pyrope-majorite garnets (Py(62)Mj(38) and Py(50)Mj(50)) to 9 GPa. *Physics of the Earth and Planetary Interiors* 120: 153–163.

Liu LG (1976) Orthorhombic perovskite phases observed in olivine, pyroxene and garnet at high-pressures and temperatures. *Physics of the Earth and Planetary Interiors* 11: 289–298.

Liu W, Kung J, and Li B (2005) Elasticity of San Carlos olivine to 8 GPa and 1073 K. *Geophysical Research Letters* 32: L16301 (doi:10.1029/2005GL023453).

Mainprice D, Barruol G, and Ismail WB (2000) The seismic anisotropy of the Earth's mantle: From single crystal to polycrystal. In: Karato SI, Forte A, Liebermann R, Masters G, and Stixrude L (eds.) *Earth's Deep Interior: Mineral Physics and Tomography from the Atomic to the Global Scale*. Washington, DC: American Geophysical Union.

Mainprice D, Tommasi A, Couvy H, Cordier P, and Frost DJ (2005) Pressure sensitivity of olivine slip systems and seismic anisotropy of Earth's upper mantle. *Nature* 433: 731–733.

Masters G, Laske G, Bolton H, and Dziewonski A (2000) The relative behavior of shear velocity, bulk sound speed, and compressional velocity in the mantle: Implications for chemical and thermal structure. In: Karato SI, Forte A, Liebermann R, Masters G, and Stixrude L (eds.) *Earth's Deep Interior: Mineral Physics and Tomography from the Atomic to the Global Scale*, pp. 63–88. Washington, DC: American Geophysical Union.

Masters TG (1979) Observational constraints on the chemical and thermal structure of the Earth's deep interior. *Geophysical Journal of the Royal Astronomical Society* 57: 507–534.

Matsukage KN, Jing Z, and Karato S (2005) Density of hydrous silicate melt at the conditions of Earth's deep upper mantle. *Nature* 438: 488–491.

McKenzie D and Bickle MJ (1988) The volume and composition of melt generated by extension of the lithosphere. *Journal of Petrology* 29: 625–679.

Mei S and Kohlstedt DL (2000a) Influence of water on plastic deformation of olivine aggregates 1. Diffusion creep regime. *Journal of Geophysical Research, Solid Earth* 105: 21457–21469.

Mei S and Kohlstedt DL (2000b) Influence of water on plastic deformation of olivine aggregates 2. Dislocation creep regime. *Journal of Geophysical Research, Solid Earth* 105: 21471–21481.

Merkel S, Kubo A, Miyagi L, *et al.* (2006) Plastic deformation of $MgGeO_3$ post-perovskite at lower mantle pressures. *Science* 311: 644–646.

Montagner JP and Anderson DL (1989) Constrained reference mantle model. *Physics of the Earth and Planetary Interiors* 58: 205–227.

Montagner JP and Guillot L (2002) Seismic anisotropy and global geodynamics. In: Karato S-i and Wenk H-R (eds.) *Plastic Deformation of Minerals and Rocks,* pp. 353–385.

Montagner JP and Kennett BLN (1996) How to reconcile body-wave and normal-mode reference Earth models. *Geophysical Journal International* 125: 229–248.

Morelli A, Dziewonski AM, and Woodhouse JH (1986) Anisotropy of the inner core inferred from PKIKP travel times. *Geophysical Research Letters* 13: 1545–1548.
Murakami M, Hirose K, Kawamura K, Sata N, and Ohishi Y (2004) Post-perovskite phase transition in $MgSiO_3$. *Science* 304: 855–858.
Nakagawa T and Buffett BA (2005) Mass transport mechanism between the upper and lower mantle in numerical simulations of thermochemical mantle convection with multicomponent phase changes. *Earth and Planetary Science Letters* 230: 11–27.
Nataf HC, Nakanishi I, and Anderson DL (1986) Measurements of mantle wave velocities and inversion for lateral heterogeneities and anisotropy.3. Inversion. *Journal of Geophysical Research, Solid Earth and Planets* 91: 7261–7307.
Nguyen JH and Holmes NC (2004) Melting of iron at the physical conditions of the Earth's core. *Nature* 427: 339–342.
Ni SD, Tan E, Gurnis M, and Helnberger D (2002) Sharp sides to the African superplume. *Science* 296: 1850–1852.
Nishimura CE and Forsyth DW (1989) The anisotropic structure of the upper mantle in the Pacific. *Geophysical Journal, Oxford* 96: 203–229.
Obayashi M, Sugioka H, Yoshimitsu J, and Fukao Y (2006) High temperature anomalies oceanward of subducting slabs at the 410-km discontinuity. *Earth and Planetary Science Letters* 243: 149–158.
Oganov AR, Brodholt JP, and Price GD (2001) The elastic constants of $MgSiO_3$ perovskite at pressures and temperatures of the Earth's mantle. *Nature* 411: 934–937.
Oganov AR and Ono S (2004) Theoretical and experimental evidence for a post-perovskite phase of $MgSiO_3$ in Earth's D″ layer. *Nature* 430: 445–448.
Ono S, Ohishi Y, and Mibe K (2004) Phase transition of Ca-perovskite and stability of Al-bearing Mg-perovskite in the lower mantle. *American Mineralogist* 89: 1480–1485.
Pacalo REG and Gasparik T (1990) Reversals of the orthoenstatite–clinoenstatite transition at high-pressures and high-temperatures. *Journal of Geophysical Research, Solid Earth and Planets* 95: 15853–15858.
Panning M and Romanowicz B (2004) Inferences on flow at the base of Earth's mantle based on seismic anisotropy. *Science* 303: 351–353.
Pasternak MP, Taylor RD, Jeanloz R, Li X, Nguyen JH, and McCammon CA (1997) High pressure collapse of magnetism in $Fe^{0.94}O$: Mossbauer spectroscopy beyond 100 GPa. *Physical Review Letters* 79: 5046–5049.
Paulssen H (1988) Evidence for a sharp 670-km discontinuity as inferred from P- to S-converted waves. *Journal of Geophysical Research, Solid Earth and Planets* 93: 10489–10500.
Poirier J-P (1994) Light elements in the Earth's outer core: A critical review. *Physics of the Earth and Planetary Interiors* 85: 319–337.
Revenaugh J and Jordan TH (1991a) Mantle layering from SCS reverberations.2. The transition zone. *Journal of Geophysical Research, Solid Earth* 96: 19763–19780.
Revenaugh J and Jordan TH (1991b) Mantle layering from SCS reverberations.3. The upper mantle. *Journal of Geophysical Research, Solid Earth* 96: 19781–19810.
Revenaugh J and Sipkin SA (1994) Seismic evidence for silicate melt atop the 410 km mantle discontinuity. *Nature* 369: 474–476.
Ribe NM (1989) Seismic anisotropy and mantle flow. *Journal of Geophysical Research, Solid Earth and Planets* 94: 4213–4223.
Rigden SM, Gwanmesia GD, Fitzgerald JD, Jackson L, and Liebermann RC (1991) Spinel elasticity and seismic structure of the transition zone of the mantle. *Nature* 354: 143–145.
Ringwood AE (1969) Composition and evolution of the upper mantle. In: Hart PJ (ed.) *The Earth's Crust and Upper Mantle*, pp. 1–17. Washington, DC: American Geophysical Union.
Ringwood AE and Major A (1970) The system Mg_2SiO_4–Fe_2SiO_4 at high pressures and temperatures. *Physics of the Earth and Planetary Interiors* 3: 89–108.
Ritsema J and van Heijst HJ (2002) Constraints on the correlation of P- and S-wave velocity heterogeneity in the mantle from P, PP, PPP and PKPab traveltimes. *Geophysical Journal International* 149: 482–489.
Robertson GS and Woodhouse JH (1996) Ratio of relative S to P velocity heterogeneity in the lower mantle. *Journal of Geophysical Research* 101: 20041–020052.
Romanowicz B (1995) A global tomographic model of shear attenuation in the upper-mantle. *Journal of Geophysical Research, Solid Earth* 100: 12375–12394.
Romanowicz B (1998) Attenuation tomography of the Earth's mantle: A review of current status. *Pure and Applied Geophysics* 153: 257–272.
Romanowicz B (2003) Global mantle tomography: Progress status in the past 10 years. *Annual Review of Earth and Planetary Sciences* 31: 303–328.
Roth EG, Wiens DA, and Zhao D (2000) An empirical relationship between seismic attenuation and velocity anomalies in the upper mantle. *Geophysical Research Letters* 27: 601–604.
Russo RM and Silver PG (1994) Trench-parallel flow beneath the nazca plate from seismic anisotropy. *Science* 263: 1105–1111.
Sakamaki T, Suzuki A, and Ohtani E (2006) Stability of hydrous melt at the base of the Earth's upper mantle. *Nature* 439: 192–194.
Sato H, Sacks IS, and Murase T (1989) The use of laboratory velocity data for estimating temperature and partial melt fraction in the low-velocity zone – Comparison with heat-flow and electrical-conductivity studies. *Journal of Geophysical Research, Solid Earth and Planets* 94: 5689–5704.
Selby ND and Woodhouse JH (2002) The Q structure of the upper mantle: Constraints from Rayleigh wave amplitudes. *Journal of Geophysical Research, Solid Earth* 107: 2097 (doi:10.1029/2001JB000257).
Shearer PM (1990) Seismic imaging of upper-mantle structure with new evidence for a 520-km discontinuity. *Nature* 344: 121–126.
Shim SH, Duffy TS, and Shen G (2001) The post-spinel transformation in Mg_2SiO_4 and its relation to the 660-km seismic discontinuity. *Nature* 411: 571–574.
Shim SH, Jeanloz R, and Duffy TS (2002) Tetragonal structure of $CaSiO_3$ perovskite above 20 GPa. *Geophysical Research Letters* 29: 2166 (doi:10.1029/2002GL016148).
Sidorin I, Gurnis M, and Helmberger DV (1999) Evidence for a ubiquitous seismic discontinuity at the base of the mantle. *Science* 286: 1326–1331.
Silver PG (1996) Seismic anisotropy beneath the continents: Probing the depths of geology. *Annual Review of Earth and Planetary Sciences* 24: 385–432.
Simmons NA and Gurrola H (2000) Multiple seismic discontinuities near the base of the transition zone in the Earth's mantle. *Nature* 405: 559–562.
Sinogeikin SV and Bass JD (2002) Elasticity of majorite and a majorite-pyrope solid solution to high pressure: Implications for the transition zone. *Geophysical Research Letters* 29: 1017 (doi:10.1029/2001GL013937).
Sinogeikin SV, Bass JD, and Katsura T (2003) Single-crystal elasticity of ringwoodite to high pressures and high temperatures: Implications for 520 km seismic discontinuity. *Physics of the Earth and Planetary Interiors* 136: 41–66.

Sobolev SV, Zeyen H, Stoll G, and Friederike WAF (1996) Upper mantle temperatures from teleseismic tomography of French Massif Central including effects of composition, mineral reactions, anharmonicity, anelasticity and partial melt. *Earth and Planetary Science Letters* 139: 147–163.
Solomatov VS and Stevenson DJ (1994) Can sharp seismic discontinuities be caused by nonequilibrium phase-transformations. *Earth and Planetary Science Letters* 125: 267–279.
Song TRA, Helmberger DV, and Grand SP (2004) Low-velocity zone atop the 410-km seismic discontinuity in the northwestern United States. *Nature* 427: 530–533.
Speziale S, Fuming J, and Duffy TS (2005a) Compositional dependence of the elastic wave velocities of mantle minerals: Implications for seismic properties of mantle rocks. In: Matas J, van der Hilst RD, Bass JD, and Trampert J (eds.) *Earth's Deep Mantle: Structure, Composition, and Evolution*, pp. 301–320. Washington, DC: American Geophysical Union.
Speziale S, Milner A, Lee VE, Clark SM, Pasternak MP, and Jeanloz R (2005b) Iron spin transition in Earth's mantle. *Proceedings of the National Academy of Sciences of the United States of America* 102: 17918–17922.
Stackhouse S, Brodholt JP, Wookey J, Kendall J-M, and Price GD (2005) The effect of temperature on the seismic anisotropy of the perovskite and post-perovskite polymorphs of $MgSiO_3$. *Earth and Planetary Science Letters* 230: 1–10.
Steinle-Neumann G, Stixrude L, and Cohen RE (2002) Physical properties of iron in the inner core. In: Dehant V, Creager KC, Karato S-i, and Zatman S (eds.) *Core Structure, Dynamics, and Rotation*, pp. 137–161. Washington, DC: American Geophysical Union.
Steinle-Neumann G, Stixrude L, Cohen RE, and Glseren O (2001) Elasticity of iron at the temperature of the Earth's inner core. *Nature* 413: 57–60.
Stevenson DJ (1981) Models of the Earths core. *Science* 214: 611–619.
Stixrude L (1997) Structure and sharpness of phase transitions and mantle discontinuities. *Journal of Geophysical Research, Solid Earth* 102: 14835–14852.
Stixrude L (1998) Elastic constants and anisotropy of $MgSiO_3$ perovskite, periclase, and SiO_2 at high pressure. In: Gurnis M, Wysession ME, Knittle E, and Buffett BA (eds.) *The Core–Mantle Boundary Region*, pp. 83–96. Washington, DC: American Geophysical Union.
Stixrude L and Cohen RE (1995) High pressure elasticity of iron and anisotropy of Earth's inner core. *Science* 267: 1972–1975.
Stixrude L, Cohen RE, Yu R, and Krakauer H (1996) Prediction of phase transition in $CaSiO_3$ perovskite and implications for lower mantle structure. *American Mineralogist* 81: 1293–1296.
Stixrude L and Karki B (2005) Structure and freezing of $MgSiO_3$ liquid in Earth's lower mantle. *Science* 310: 297–299.
Stixrude L and Lithgow-Bertelloni C (2005a) Mineralogy and elasticity of the oceanic upper mantle: Origin of the low-velocity zone. *Journal of Geophysical Research, Solid Earth* 110: B03204 (doi:10.1029/2004JB002965).
Stixrude L and Lithgow-Bertelloni C (2005b) Thermodynamics of mantle minerals. I: Physical properties. *Geophysical Journal International* 162: 610–632.
Stixrude L and Lithgow-Bertelloni C (2007) Influence of phase transformations on lateral heterogeneity and dynamics in Earth's mantle. *Earth and Planetary Science Letters,* (submitted).
Stixrude L, Lithgow-Bertelloni C, Kiefer B, and Fumagalli P (2007) Phase stability and shear softening in $CaSiO_3$ perovskite at high pressure. *Physical Review B,*75: 024108.
Su WJ and Dziewonski AM (1995) Inner-core anisotropy in 3 Dimensions. *Journal of Geophysical Research, Solid Earth* 100: 9831–9852.
Su Wj and Dziewonski AM (1997) Simultaneous inversion for 3-D variations in shear and bulk velocity in the mantle. *Physics of the Earth and Planetary Interiors* 100: 135–156.
Söderlind P, Moriarty JA, and Wills JM (1996) First-principles theory of iron up to earth-core pressures: Structural, vibrational, and elastic properties. *Physical Review B* 53: 14063–14072.
Takafuji N, Hirose K, Mitome M, and Bando Y (2005) Solubilities of O and Si in liquid iron in equilibrium with (Mg,Fe)SiO_3 perovskite and the light elements in the core. *Geophysical Research Letters* 32: L06313 (doi:10.1029/2005GL022773).
Tanaka S and Hamaguchi H (1997) Degree one heterogeneity and hemispherical variation of anisotropy in the inner core from PKP(BC)-PKP(DF) times. *Journal of Geophysical Research, Solid Earth* 102: 2925–2938.
Tanimoto T and Anderson DL (1984) Mapping convection in the mantle. *Geophysical Research Letters* 11: 287–290.
Trampert J and van Heijst HJ (2002) Global azimuthal anisotropy in the transition zone. *Science* 296: 1297–1299.
Tsuchiya T, Tsuchiya J, Umemoto K, and Wentzcovitch RM (2004a) Phase transition in $MgSiO_3$ perovskite in the Earth's lower mantle. *Earth and Planetary Science Letters* 224: 241–248.
Tsuchiya T, Tsuchiya J, Umemoto K, Wentzcovitch RM, *et al.* (2004b) Elasticity of post-perovskite $MgSiO_3$. *Geophysical Research Letters* 31: L14603 (doi:10.1029/2004GL020278).
Tsuchiya T, Wentzcovitch RM, da Silva CRS, and de Gironcoli S (2006) Spin transition in magnesiowüstite in Earth's lower mantle. *Physical Review Letters* 96: 198501.
van der Meijde M, Marone F, Giardini D, and van der Lee S (2003) Seismic evidence for water deep in Earth's upper mantle. *Science* 300: 1556–1558.
van der Meijde M, van der Lee S, and Giardini D (2005) Seismic discontinuities in the Mediterranean mantle. *Physics of the Earth and Planetary Interiors* 148: 233–250.
van Hunen J, Zhong S, Shapiro NM, and Ritzwoller MH (2005) New evidence for dislocation creep from 3-D geodynamic modeling of the Pacific upper mantle structure. *Earth and Planetary Science Letters* 238: 146–155.
Vasco D and Johnson LR (1998) Whole Earth structure estimated from seismic arrival times. *Journal of Geophysical Research* 103: 2633–2672.
Vinnik L, Kato M, and Kawakatsu H (2001) Search for seismic discontinuities in the lower mantle. *Geophysical Journal International* 147: 41–56.
Vocadlo L, Alfe D, Gillan MJ, Wood IG, Brodholt JP, and Price GD (2003) Possible thermal and chemical stabilization of body-centred-cubic iron in the Earth's core. *Nature* 424: 536–539.
Weertman J (1970) Creep strength of Earth's mantle. *Reviews of Geophysics and Space Physics* 8: 145.
Weidner DJ and Wang YB (1998) Chemical- and Clapeyron-induced buoyancy at the 660 km discontinuity. *Journal of Geophysical Research, Solid Earth* 103: 7431–7441.
Wentzcovitch RM, Karki BB, Cococcioni M, and de Gironcoli S (2004) Thermoelastic properties of $MgSiO_3$-perovskite: Insights on the nature of the Earth's lower mantle. *Physical Review Letters* 92: 018501.
Wentzcovitch RM, Tsuchiya T, and Tsuchiya J (2006) $MgSiO_3$ postperovskite at D″ conditions. *Proceedings of the National Academy of Sciences of the United States of America* 103: 543–546.
Williams Q and Garnero EJ (1996) Seismic evidence for partial melt at the base of Earth's mantle. *Science* 273: 1528.
Wood BJ (1990) Postspinel transformations and the width of the 670-km discontinuity – A comment on postspinel

transformations in the system Mg_2SiO_4–Fe_2SiO_4 and some geophysical implications by Ito,E. And Takahashi,E. *Journal of Geophysical Research, Solid Earth and Planets* 95: 12681–12685.
Wood BJ (1995) The effect of H_2O on the 410-kilometer seismic discontinuity. *Science* 268: 74–76.
Woodhouse JH, Giardini D, and Li X-D (1986) Evidence for inner core anisotropy from free oscillations. *Geophysical Research Letters* 13: 1549–1552.
Woodland AB (1998) The orthorhombic to high-P monoclinic phase transition in Mg–Fe pyroxenes: Can it produce a seismic discontinuity? *Geophysical Research Letters* 25: 1241–1244.
Workman RK and Hart SR (2005) Major and trace element composition of the depleted MORB mantle (DMM). *Earth and Planetary Science Letters* 231: 53–72.
Wysession ME, Lay T, Revenaugh J, *et al.* (1998) The D″ discontinuity and its implicatinos. In: Gurnis M, Wysession ME, Knittle E, and Buffett BA (eds.) *The Core–Mantle Boundary Region*. Washington, DC: American Geophysical Union.
Xie SX and Tackley PJ (2004) Evolution of helium and argon isotopes in a convecting mantle. *Physics of the Earth and Planetary Interiors* 146: 417–439.
Young CJ and Lay T (1987) The core–mantle boundary. *Annual Review of Earth and Planetary Sciences* 15: 25–46.
Zha C-s, Duffy TS, Ho-kwang M, Downs RT, Hemley RJ, and Weidner DJ (1997) Single-crystal elasticity of beta-Mg_2SiO_4 to the pressure of the 410 km seismic discontinuity in the Earth's mantle. *Earth and Planetary Science Letters* 147: E9–E15.